Eur. Phys. J. Plus (2024) 139:1064
https://doi.org/10.1140/epjp/s13360-024-05845-1

THE EUROPEAN PHYSICAL JOURNAL PLUS

Regular Article

Dynamics of a delayed HIV infection model with cell-to-cell transmission and homeostatic proliferation

Xia Wang[1], **Yue Wang**[1], **Yueping Dong**[2], **Libin Rong**[3,a]

[1] College of Mathematics and Information Science, Xinyang Normal University, Xinyang 464000, China
[2] School of Mathematics and Statistics and Hubei Key Laboratory of Mathematical Sciences, Central China Normal University, Wuhan 430079, China
[3] Department of Mathematics, University of Florida, Gainesville, FL 32611, USA

Received: 17 October 2024 / Accepted: 15 November 2024

Abstract Homeostatic proliferation plays an important role in cell proliferation. In this paper, we developed a delayed HIV infection model incorporating two modes of infection along with homeostatic proliferation. We showed the positivity of the solution and the existence of the steady state for the dimensionless model. We derived the conditions for local stability and the occurrence of Hopf bifurcation at the infected steady state. We also established the direction and stability of Hopf bifurcation by using the center manifold theorem and normal form method. Numerical simulations were conducted to demonstrate the analytical results and explore the effect of delays on the virus dynamics. Our findings indicate that homeostatic proliferation or an intracellular time delay can destabilize the infected steady state. However, cell-to-cell transmission alone cannot induce a stability switch in the infected steady state. Furthermore, as the intracellular time delay or the homeostatic proliferation rate increases, the time required for the model to reach an infected steady state also increases.

1 Introduction

Infectious diseases continue to pose a significant threat to global public health, and among these, the human immunodeficiency virus (HIV) stands out as particularly detrimental. As a retrovirus, HIV primarily targets the crucial CD4+ T cells in the human immune system. According to the World Health Organization (WHO), HIV has claimed over 40.4 million lives to date. By the end of 2022, it is estimated that around 39 million people were living with HIV, with two-thirds of them (approximately 25.6 million) located in the African region [1]. Since its initial identification in 1981, the global community has been relentless in its battle against HIV. As awareness of its devastating effects on human health has grown, extensive research has been conducted to understand the dynamic behavior of this virus.

Many existing HIV models focus solely on cell-free virus infection [2–6] and incorporate aspects such as delays, age structure, and latency. These models often overlook cell-to-cell transmission, which might be more efficient in transmitting the virus because it can transmit several virions each time and the virus is not exposed to the neutralization of antibodies [7, 8]. Given the importance of understanding HIV's spread, it is essential to consider the role of cell-to-cell transmission. In recent years, many models have begun to include this form of transmission [9–12]. For instance, Wang et al. [10] examined an HIV latent infection model that features cell-to-cell transmission, assessing how time delays and the fraction of infection contributing to these delays affect virus dynamics. They also evaluated the relative contributions of both transmission modes to the HIV population. Furthermore, viral infection is a complex process that does not occur instantaneously. For example, the virus enters target cells, followed by reverse transcription, integration, transcription, and translation [3]. Therefore, introducing delay(s) to capture the temporal dynamics in viral infection and other diseases aligns more closely with real-world observations [2, 13, 14].

Cell proliferation plays a crucial role in the infection of HIV and should not be overlooked. Research highlighted in [15] has demonstrated the significant impact of CD4+ T cells in primary viral infections. Thus, varying levels of CD4+ T cells may either promote or inhibit virus replication during HIV transmission. Previous studies of HIV within-host models have typically focused on viral infection or clearance, considering only parameter variations and overlooking initial viral loads or changes in CD4+ T cell counts during transmission [16]. In this paper, we focus primarily on the homeostatic proliferation of CD4+ T cells, which provides HIV additional opportunities to infect through free virus particles by replenishing the pool of target cells. In the absence of specific antigens, CD4+ T cell division in depleted lymphoid tissues is thought to be driven by the presence of foreign antigens [17, 18]. Fan et al. explored an acute phase model that relies solely on healthy CD4+ T cells, illustrating the body's regulatory mechanism to maintain CD4+ T cell population [19].

[a] e-mail: libinrong@ufl.edu (corresponding author)

Published online: 04 December 2024

Studies have shown that in the context of reduced lymphoid cells caused by HIV, the homeostatic proliferation of CD4+ T cells is primarily driven by viral load. This increase in viral load not only consumes CD4+ T cells but also leads to the recruitment of immature CD4+ T cells into a proliferation pool [20]. Therefore, in the presence of HIV, this regulatory mechanism is influenced by both the intensity of the viral load and the size of the CD4+ T cell population. Many studies found that the production of new CD4+ T cells and macrophages from the thymus, bone marrow, and other sources typically remains constant. However, HIV and other pathogens can induce the proliferation of immune cells [21–24], necessitating a consideration of homeostatic proliferation in response to infection.

The structure of this article is as follows. In Sect. 2, we construct a delayed HIV infection model that incorporates homeostatic proliferation and cell-to-cell transmission. We determine the basic reproduction number of the model and the dimensionless system. In Sect. 3, we study the local stability of all the steady states of the dimensionless model and analyze the existence of Hopf bifurcation at the infected steady state. The direction and stability of Hopf bifurcation are determined using the center manifold theorem and normal form theory in Sect. 4. In Sect. 5, numerical simulations are used to illustrate the analytical results. Finally, the paper concludes with a brief summary and discussion.

2 Mathematical model

2.1 Model formulation

We have included homeostatic proliferation and cell-to-cell transmission in the model, which resulted in the following delayed HIV infection model with two modes of transmission.

$$\begin{aligned}\frac{\mathrm{d}T(t)}{\mathrm{d}t} &= \Lambda + \frac{\varepsilon}{M+V(t)}T(t)V(t) - kT(t)V(t) - \beta T(t)I(t) - d_1T(t),\\ \frac{\mathrm{d}I(t)}{\mathrm{d}t} &= kT(t-\tau)V(t-\tau)e^{-\delta\tau} + \beta T(t-\tau)I(t-\tau)e^{-\delta\tau} - d_2I(t),\\ \frac{\mathrm{d}V(t)}{\mathrm{d}t} &= pI(t) - d_3V(t),\end{aligned} \tag{2.1}$$

where $T(t)$, $I(t)$, and $V(t)$ represent the concentrations of uninfected CD4+ T cells, infected cells, and free virus at time t, respectively. The time τ represents the intracellular delay, which is the time it takes for uninfected CD4+ T cells to become productively infected after coming into contact with the virus. The model assumes that uninfected CD4+ T cells are produced at a rate Λ, and die at a rate d_1. Healthy CD4+ T cells are infected by free viruses at a rate k and through direct cell-to-cell transmission at a rate β. Since the time delay between viral entry and viral production is independent of the transmission mode, we apply the same delay for kTV and βTI, collectively referred to as the intracellular delay. The parameter p indicates the rate at which new virions are produced by infected cells. The death rate of infected cells is denoted by d_2, and d_3 is the rate of viral clearance. The death rate of infected cells that have not begun to produce viruses is δ, and $e^{-\delta\tau}$ represents the survival probability of these infected cells.

The term $\frac{\varepsilon}{M+V(t)}T(t)V(t)$ describes the homeostatic proliferation due to the immune response, as detailed in [25]. Specifically, the homeostatic proliferation of CD4+ T cells is triggered by the presence of the virus and the consequent decrease in the number of uninfected CD4+ T cells. Here, ε represents the maximum growth rate, and M is the half-velocity constant of growth. We define the function $F(V) = \frac{\varepsilon}{M+V}V$, which satisfies $F(0) = 0$, $F'(V) > 0$, and $\lim\limits_{V\to\infty} F(V) = \varepsilon$. Thus, this saturated term vanishes when no virions are present in the model. The basic dynamics of the model align with those of the general virus model. Furthermore, as the virus population grows, the immune system of the infected host replenishes the CD4+ T cells to compensate for what is consumed in-host, with the maximum growth rate given by εT. Although the growth rate of this term is limited, homeostatic proliferation significantly impacts the dynamics of the model. When cells undergo pathological changes, their concentration does not sharply increase or grow indefinitely over time but instead varies within a limited range. Therefore, to maintain biological relevance, we assume that the maximum growth rate of uninfected cells is less than their death rate, meaning that $\varepsilon < d_1$ [27].

Model (2.1) always has the steady state $P_0 = (\frac{\Lambda}{d_1}, 0, 0)$. Through the next-generation matrix method [28], we obtain

$$\mathbb{F}\mathbb{V}^{-1} = \begin{pmatrix} \frac{pk\Lambda}{d_1d_2d_3}e^{-\delta\tau} + \frac{\beta\Lambda}{d_1d_2}e^{-\delta\tau} & \frac{k\Lambda}{d_1d_3}e^{-\delta\tau} \\ 0 & 0 \end{pmatrix}.$$

The basic reproduction number is given by $\rho(\mathbb{F}\mathbb{V}^{-1})$, where ρ denotes the spectral radius of the next-generation matrix. Thus, we have

$$R_0 = \frac{pk\Lambda}{d_1d_2d_3}e^{-\delta\tau} + \frac{\beta\Lambda}{d_1d_2}e^{-\delta\tau}.$$

R_0 refers to the number of secondary infections caused by a single infected cell (or virus) in a completely susceptible environment. The term $\frac{pk\Lambda}{d_1d_2d_3}e^{-\delta\tau}$ represents the basic reproduction number for the model with cell-free infection, while $\frac{\beta\Lambda}{d_1d_2}e^{-\delta\tau}$ represents the basic reproduction number for the model with cell-to-cell transmission.

2.2 Positivity and boundedness of solution

The following result shows that the solution $(T(t), I(t), V(t))$ of model (2.1) remains nonnegative and boundedness.

Theorem 2.1 *Under the given initial conditions, all solutions of model (2.1) are positive and ultimately bounded for all $t > 0$.*

Proof We first show that $T(t) > 0$ for all $t > 0$. Assume that there exists a $t_1 > 0$ such that $T(t_1) = 0,\ T(t) > 0,\ t \in [0, t_1)$. Thus, $\dot{T}(t_1) \leq 0$. From the first equation of model (2.1), we have $\dot{T}(t_1) = \Lambda > 0$, which is a contradiction. This implies that $T(t) > 0$ for all $t > 0$.

Next, we prove that $I(t) > 0,\ V(t) > 0$ for all $t > 0$. Assume that there exist a $t_2 > 0$ such that $\min\{I(t_2),\ V(t_2)\} = 0$.

If $I(t_2) = 0$, $I(t) > 0$ for $t \in [0, t_2)$ and $V(t) > 0,\ t \in [0, t_2]$, then $\dot{I}(t_2) \leq 0$. We have

$$\frac{\mathrm{d}I(t_2)}{\mathrm{d}t} = kT(t_2 - \tau)V(t_2 - \tau)e^{-\delta\tau} + \beta T(t_2 - \tau)I(t_2 - \tau)e^{-\delta\tau}.$$

When $t_2 - \tau \in [0, t_2)$, we have $\dot{I}(t_2) > 0$, which is a contradiction. This implies that $I(t) > 0$ for all $t > 0$.

By the last equation of model (2.1), we have

$$V(t) = V_0 e^{-d_3 t} + \int_0^t pI(\xi)e^{-d_3(t-\xi)}\mathrm{d}\xi > 0.$$

Thus, $T(t) > 0,\ I(t) > 0,\ V(t) > 0$ for all $t > 0$. Similarly, we can prove that $V(t_2) = 0$, $V(t) > 0$ for $t \in [0, t_2)$, $I(t) > 0$, $t \in [0, t_2]$ and $I(t_2) = V(t_2) = 0$, $I(t)$, $V(t) > 0$ for $t \in [0, t_2)$ are possible using the same method.

In conclusion, $T(t)$, $I(t)$, $V(t) > 0$ for all $t > 0$.

The boundedness of the model is proved below. Define $\mathcal{N}(t) = T(t) + I(t + \tau)e^{\delta\tau}$. We have

$$\begin{aligned}
\frac{\mathrm{d}\mathcal{N}(t)}{\mathrm{d}t} &\leq \Lambda + \frac{\varepsilon}{M + V(t)}T(t)V(t) - d_1 T(t) - d_2 I(t + \tau)e^{\delta\tau} \\
&\leq \Lambda + \varepsilon T(t) - d_1 T(t) - d_2 I(t + \tau)e^{\delta\tau} \\
&\leq \Lambda - (d_1 - \varepsilon)T(t) - d_2 I(t + \tau)e^{\delta\tau} \\
&\leq \Lambda - \mathrm{d}\mathcal{N}(t).
\end{aligned}$$

Thus, $\lim\limits_{t\to\infty} \sup \mathcal{N}(t) \leq \frac{\Lambda}{d}$ and $d = \min\{d_1 - \varepsilon, d_2\}$. Moreover, we obtain $\lim\limits_{t\to\infty} \sup V(t) \leq \frac{\Lambda p}{dd_3}$. □

Therefore, Υ defined dy

$$\Upsilon = \left\{(T(t), I(t), V(t)) \in R_+^3 : 0 < T(t) + I(t) \leq \frac{\Lambda}{d},\ V(t) \leq \frac{\Lambda p}{dd_3}\right\}$$

is a globally attractive and positively invariant subset of model (2.1).

2.3 Dimensionless model

To reduce the parameter space, model (2.1) can be reconstructed to a dimensionless form. Let

$$\begin{aligned}
&\tilde{T}(\tilde{t}) = \frac{T(t)}{T^*},\quad \tilde{I}(\tilde{t}) = \frac{I(t)}{I^*},\quad \tilde{V}(\tilde{t}) = \frac{V(t)}{V^*},\quad \tilde{t} = \frac{t}{t^*},\quad \tilde{\tau} = \frac{\tau}{\tau^*}, \\
&T^* = \frac{d_2 d_3}{(pk + \beta d_3)e^{-\delta\tau}},\quad I^* = \frac{d_1 d_3}{pk},\quad V^* = \frac{d_1}{k},\quad t^* = \tau^* = \frac{1}{d_1}.
\end{aligned}$$

To simplify, we remove the symbol $\sim$, which leads to

$$\begin{aligned}
\frac{\mathrm{d}T(t)}{\mathrm{d}t} &= R_0 + \frac{R_m}{1 + \beta_1 V(t)}T(t)V(t) - T(t)V(t) - \beta_2 T(t)I(t) - T(t), \\
\frac{\mathrm{d}I(t)}{\mathrm{d}t} &= \alpha_1 T(t - \tau)V(t - \tau) + \alpha_2 T(t - \tau)I(t - \tau) - \alpha_3 I(t), \\
\frac{\mathrm{d}V(t)}{\mathrm{d}t} &= \alpha_4[I(t) - V(t)],
\end{aligned} \tag{2.2}$$

where

$$\begin{aligned}
&R_0 = \frac{pk\Lambda}{d_1 d_2 d_3}e^{-\delta\tau} + \frac{\beta\Lambda}{d_1 d_2}e^{-\delta\tau},\quad R_m = \frac{\varepsilon}{Mk},\quad \beta_1 = \frac{d_1}{Mk},\quad \beta_2 = \frac{\beta d_3}{pk}, \\
&\alpha_1 = \frac{pkd_2}{d_1(pk + \beta d_3)},\quad \alpha_2 = \frac{\beta d_2 d_3}{d_1(pk + \beta d_3)},\quad \alpha_3 = \frac{d_2}{d_1},\quad \alpha_4 = \frac{d_3}{d_1}.
\end{aligned}$$

Each new parameter is positive, reflecting the positivity of the original parameters. The properties of the transformed model remain unchanged, ensuring that the solutions of model (2.2) are positive and uniformly bounded. Moreover, we typically fix the values of β_1, β_2, α_1, α_2, α_3, and α_4 while exploring variations in R_0 and R_m. Here, $\alpha_1 + \alpha_2 = \alpha_3$ and $\alpha_1\beta_2 = \alpha_2$. R_0 represents the basic reproduction number of model (2.1), derived using the next-generation matrix method, while R_m denotes a new reproduction number introduced by incorporating the saturated term.

Let's define the Banach space as follows:

$$\Omega_+ = \{\varphi = (\varphi_1, \varphi_2, \varphi_3) \in \Omega : \varphi_i(\theta) \geq 0 \quad \text{for all} \quad \theta \in [-\tau, 0],\ i = 1, 2, 3\}.$$

The Banach space of continuous functions mapping the interval $[-\tau, 0]$ to R^3_+ is defined by $\varphi : [-\tau, 0] \to R^3_+$. The initial conditions of model (2.2) is

$$T(\theta) = \varphi_1(\theta),\ \ I(\theta) = \varphi_2(\theta),\ \ V(\theta) = \varphi_3(\theta),\quad \theta \in [-\tau, 0], \tag{2.3}$$

where $\varphi = (\varphi_1, \varphi_2, \varphi_3) \in \Omega_+$.

3 Stability analysis

3.1 Existence of the steady state

Model (2.2) always has an infection-free steady state $E_0 = (R_0, 0, 0)$. For the other steady states, we use the same approach as in [16] and the components of equilibrium satisfy

$$\begin{aligned} &R_0 + \frac{R_m}{1+\beta_1 V} TV - TV - \beta_2 TI - T = 0,\\ &\alpha_1 TV + \alpha_2 TI - \alpha_3 I = 0,\\ &\alpha_4(I - V) = 0. \end{aligned} \tag{3.1}$$

Starting with the equilibrium equations (3.1), we use the last equation to deduce that $I = V$. This leads to the infection-free steady state E_0 if $I = V = 0$. When $I = V \neq 0$, substituting this condition in the second equation yields:

$$\alpha_1 T + \alpha_2 T = \alpha_3, \quad T = \frac{\alpha_3}{\alpha_1 + \alpha_2} = 1.$$

From this equation, we can derive a formula for V, specifically:

$$c_1 V^2 + c_2 V + c_3 = 0, \tag{3.2}$$

where

$$c_1 = \beta_1(1 + \beta_2) > 0, \quad c_2 = \beta_1(1 - R_0) + 1 - R_m + \beta_2, \quad c_3 = 1 - R_0.$$

(a) If $R_0 < 1$, then $c_3 > 0$.

The condition $\Delta = c_2^2 - 4c_1c_3 \geq 0$ needs to be satisfied, which implies that all the solutions of the equation are real values.

(i) $\Delta = c_2^2 - 4c_1c_3 > 0$. This is equivalent to

$$(G + 1 + \beta_2 - R_m)^2 - 4G(1 + \beta_2) > 0,$$

where $G = \beta_1(1 - R_0)$. We have

$$\begin{aligned} &G^2 + (1 + \beta_2 - R_m)^2 + 2G(1 + \beta_2 - R_m) - 4G(1 + \beta_2)\\ &= G^2 + (1 + \beta_2 - R_m)^2 + 2G(1 + \beta_2 - R_m) - 4G(1 + \beta_2)\\ &\quad + 2G(1 + \beta_2 + R_m) - 2G(1 + \beta_2 + R_m)\\ &= G^2 - 2G(1 + \beta_2 + R_m) + (1 + \beta_2 - R_m)^2 > 0. \end{aligned}$$

It follows that

$$\left[G - \left(\sqrt{1+\beta_2} - \sqrt{R_m}\right)^2\right]\left[G - \left(\sqrt{1+\beta_2} + \sqrt{R_m}\right)^2\right] > 0.$$

Clearly, $\left(\sqrt{1+\beta_2} + \sqrt{R_m}\right)^2 > \left(\sqrt{1+\beta_2} - \sqrt{R_m}\right)^2$. Thus, $\Delta = c_2^2 - 4c_1c_3 > 0$ if and only if

$$G - \left(\sqrt{1+\beta_2} - \sqrt{R_m}\right)^2 < 0 \ \text{ or } \ G - \left(\sqrt{1+\beta_2} + \sqrt{R_m}\right)^2 > 0.$$

Then we have

$$R_0 > 1 - \frac{\left(\sqrt{1+\beta_2} - \sqrt{R_m}\right)^2}{\beta_1} \text{ or } R_0 < 1 - \frac{\left(\sqrt{1+\beta_2} + \sqrt{R_m}\right)^2}{\beta_1}.$$

The infected steady states also exist when $c_2 < 0$. The condition $1 > R_0 > 1 + \frac{1+\beta_2-R_m}{\beta_1}$ is equivalent to $1 + \beta_2 < R_m$.

Thus, we have

$$1 + \frac{1+\beta_2-R_m}{\beta_1} < R_0 < 1 - \frac{\left(\sqrt{1+\beta_2} + \sqrt{R_m}\right)^2}{\beta_1} \text{ or } B_1 < R_0 < 1,$$

where $B_1 = \max\left\{0,\ 1 - \frac{\left(\sqrt{1+\beta_2}-\sqrt{R_m}\right)^2}{\beta_1}\right\}$. Because $1 + \frac{1+\beta_2-R_m}{\beta_1} < R_0 < 1 - \frac{\left(\sqrt{1+\beta_2}+\sqrt{R_m}\right)^2}{\beta_1}$ is an empty set, this implies that there is no solution in the $(R_0,\ R_m)$ space. Under these conditions, we identify two infected steady states, E_1 and E_2.

If $B_1 < R_0 < 1$ and $1 + \beta_2 < R_m$, we have

$$E_1 = (1,\ I_1,\ V_1) = (1,\ \frac{-c_2 - \sqrt{c_2^2 - 4c_1c_3}}{2c_1},\ \frac{-c_2 - \sqrt{c_2^2 - 4c_1c_3}}{2c_1}),$$

$$E_2 = (1,\ I_2,\ V_2) = (1,\ \frac{-c_2 + \sqrt{c_2^2 - 4c_1c_3}}{2c_1},\ \frac{-c_2 + \sqrt{c_2^2 - 4c_1c_3}}{2c_1}).$$

(ii) If $\Delta = c_2^2 - 4c_1c_3 = 0$, following the same analysis as above, we have

$$\left[G - \left(\sqrt{1+\beta_2} - \sqrt{R_m}\right)^2\right]\left[G - \left(\sqrt{1+\beta_2} + \sqrt{R_m}\right)^2\right] = 0.$$

Thus,

$$R_0 = 1 - \frac{\left(\sqrt{1+\beta_2} - \sqrt{R_m}\right)^2}{\beta_1} \text{ or } R_0 = 1 - \frac{\left(\sqrt{1+\beta_2} + \sqrt{R_m}\right)^2}{\beta_1}.$$

In additon to $c_2 < 0$, we get

$$R_m > 1 + \beta_2 \text{ and } R_0 = 1 - \frac{\left(\sqrt{1+\beta_2} - \sqrt{R_m}\right)^2}{\beta_1}.$$

Under these conditions, we have a unique infected steady state E_2, which is of multiplicity 2.

(b) If $R_0 = 1$, then $c_3 = 0$. Equation (3.2) becomes

$$V(c_1V + c_2) = 0.$$

Thus, $V = 0$ or $V = -\frac{c_2}{c_1}$. Since $c_2 < 0$, we have $V = -\frac{c_2}{c_1} > 0$ and $R_m > 1 + \beta_2$. Therefore, there is a unique infected steady state E_2.

(c) If $R_0 > 1$, then $c_3 < 0$. This is the infected steady state E_2.

In summary, we present the following theorem.

Theorem 3.1 *(i) The infection-free steady state E_0 of model (2.2) always exists.*

(ii) If $R_0 = 1 - \frac{\left(\sqrt{1+\beta_2}-\sqrt{R_m}\right)^2}{\beta_1}$ and $1 + \beta_2 < R_m$ or $R_0 = 1$ and $1 + \beta_2 < R_m$ or $R_0 > 1$, then model (2.2) has a unique infected steady state E_2.

(iii) If $B_1 < R_0 < 1$ and $1 + \beta_2 < R_m$, then model (2.2) has two infected steady states E_1 and E_2.

3.2 Stability of the steady state

In this section, we examine the stability of the steady states of model (2.2) where $\tau \geq 0$. We linearize model (2.2) and derive the characteristic equation evaluated at an arbitrary steady state $\bar{E} = (\bar{T},\ \bar{I},\ \bar{V})$, which is determined by the following determinant:

$$\begin{vmatrix} \lambda + 1 + \bar{V} + \beta_2\bar{I} - \frac{R_m\bar{V}}{1+\beta_1\bar{V}} & \beta_2\bar{T} & \bar{T}\left(1 - \frac{R_m}{(1+\beta_1\bar{V})^2}\right) \\ -\alpha_1\bar{V}e^{-\lambda\tau} - \alpha_2\bar{I}e^{-\lambda\tau} & \lambda + \alpha_3 - \alpha_2\bar{T}e^{-\lambda\tau} & -\alpha_1\bar{T}e^{-\lambda\tau} \\ 0 & -\alpha_4 & \lambda + \alpha_4 \end{vmatrix} = 0. \tag{3.3}$$

Theorem 3.2 *When $R_0 < 1$, the infection-free steady state E_0 of model (2.2) is locally asymptotically stable for all $\tau \geq 0$. Otherwise, it is unstable.*

Proof For $E_0 = (R_0, 0, 0)$, the characteristic equation is

$$\begin{aligned} f(\lambda) &= (\lambda+1)(\lambda+\alpha_3)(\lambda+\alpha_4) - (\lambda+1)(\lambda+\alpha_4)\alpha_2 R_0 e^{-\lambda\tau} - (\lambda+1)\alpha_1\alpha_4 R_0 e^{-\lambda\tau} \\ &= (\lambda+1)[(\lambda+\alpha_3)(\lambda+\alpha_4) - (\lambda+\alpha_4)\alpha_2 R_0 e^{-\lambda\tau} - \alpha_1\alpha_4 R_0 e^{-\lambda\tau}] = 0. \end{aligned} \tag{3.4}$$

Our goal is to demonstrate that if the eigenvalue $\lambda_1 = x + iy$ is a solution of Eq. (3.4), then the real part $x < 0$ when $R_0 < 1$. Suppose this conclusion is incorrect, and we find that $x \geq 0$. Under this assumption, calculate equation (3.4) we get

$$\begin{aligned} 1 &= \left| \frac{\alpha_1\alpha_4 R_0 e^{-\lambda_1\tau}}{(\lambda_1+\alpha_3)(\lambda_1+\alpha_4)} + \frac{\alpha_2 R_0 e^{-\lambda_1\tau}}{\lambda_1+\alpha_3} \right| \\ &\leq \left| \frac{\alpha_1\alpha_4 R_0 e^{-\lambda_1\tau}}{(\lambda_1+\alpha_3)(\lambda_1+\alpha_4)} \right| + \left| \frac{\alpha_2 R_0 e^{-\lambda_1\tau}}{\lambda_1+\alpha_3} \right| \\ &\leq \frac{\alpha_1 R_0}{\alpha_3} + \frac{\alpha_2 R_0}{\alpha_3} \\ &= R_0. \end{aligned} \tag{3.5}$$

This leads to a contradiction. Thus, all the roots of the characteristic equation (3.4) have negative real parts. This shows that E_0 is locally asymptotically stable when $R_0 < 1$.

When $R_0 > 1$, we know that the characteristic equation $f(0) = \alpha_3\alpha_4(1 - R_0) < 0$ and $\lim_{\lambda\to+\infty} f(\lambda) = +\infty$. Therefore, there is at least one positive root such that $f(\lambda) = 0$. Thus, the infection-free steady state E_0 is unstable when $R_0 > 1$. □

The infected steady state $E_{1,2}$ is brought into the characteristic equation (3.3) and $\alpha_1 + \alpha_2 = \alpha_3$. We obtain the following characteristic equation:

$$H(\lambda, \tau) = P_1(\lambda) + P_2(\lambda)e^{-\lambda\tau} = 0, \tag{3.6}$$

where

$$P_1(\lambda) = \lambda^3 + a_2\lambda^2 + a_1\lambda + a_0, \quad P_2(\lambda) = b_2\lambda^2 + b_1\lambda + b_0$$

and

$$\begin{aligned} a_2 &= \alpha_3 + \alpha_4 + 1 + V_{1,2} + \beta_2 V_{1,2} - \frac{R_m V_{1,2}}{1+\beta_1 V_{1,2}}, \\ a_1 &= \alpha_3\alpha_4 + (\alpha_3+\alpha_4)\left(1 + V_{1,2} + \beta_2 V_{1,2} - \frac{R_m V_{1,2}}{1+\beta_1 V_{1,2}}\right), \\ a_0 &= \alpha_3\alpha_4\left(1 + V_{1,2} + \beta_2 V_{1,2} - \frac{R_m V_{1,2}}{1+\beta_1 V_{1,2}}\right), \\ b_2 &= -\alpha_2, \\ b_1 &= \alpha_3(\beta_2 V_{1,2} - \alpha_4) - \alpha_2\left(1 + V_{1,2} + \beta_2 V_{1,2} - \frac{R_m V_{1,2}}{1+\beta_1 V_{1,2}}\right), \\ b_0 &= \alpha_3\alpha_4\left(\frac{R_m V_{1,2}}{1+\beta_1 V_{1,2}} - 1 - \frac{R_m V_{1,2}}{(1+\beta_1 V_{1,2})^2}\right). \end{aligned}$$

When $\tau = 0$, the equation becomes

$$\lambda^3 + (a_2+b_2)\lambda^2 + (a_1+b_1)\lambda + a_0 + b_0 = 0. \tag{3.7}$$

Let $i\omega$ ($\omega > 0$) be a root of Eq. (3.6). We separate the real and imaginary parts and get

$$\begin{aligned} b_1\omega\sin\omega\tau + (b_0 - b_2\omega^2)\cos\omega\tau &= a_2\omega^2 - a_0, \\ (b_0 - b_2\omega^2)\sin\omega\tau - b_1\omega\cos\omega\tau &= -\omega^3 + a_1\omega. \end{aligned} \tag{3.8}$$

This leads to

$$\begin{aligned} \sin\omega\tau &= \frac{(a_2\omega^2 - a_0)b_1\omega + (b_0 - b_2\omega^2)(a_1\omega - \omega^3)}{(b_0 - b_2\omega^2)^2 + b_1^2\omega^2}, \\ \cos\omega\tau &= \frac{(\omega^3 - a_1\omega)b_2\omega + (b_0 - b_2\omega^2)(a_2\omega^2 - a_0)}{(b_0 - b_2\omega^2)^2 + b_1^2\omega^2}. \end{aligned}$$

Adding the square of each equation yields

$$\omega^6 + m\omega^4 + l\omega^2 + r = 0, \tag{3.9}$$

where

$$m = a_2^2 - 2a_1 - b_2^2, \quad l = a_1^2 + 2b_2b_0 - 2a_2a_0 - b_1^2, \quad r = a_0^2 - b_0^2.$$

Let $z = \omega^2$. Then Eq. (3.9) becomes

$$h(z) = z^3 + mz^2 + lz + r = 0. \tag{3.10}$$

Lemma 3.3 *When E_1 exists, we have $\beta_1(1+\beta_2)V_1^2 + R_0 - 1 < 0$.*

Proof From the previous discussion, we know that $R_0 < 1, c_2 < 0$ and $\Delta = c_2^2 - 4c_1c_3 > 0$ when E_1 exists. Thus, $c_3 = 1 - R_0 > 0$. We have

$$V_1 = \frac{-c_2 - \sqrt{c_2^2 - 4c_1c_3}}{2c_1}.$$

Multiplying the numerator and denominator by $-c_2 + \sqrt{c_2^2 - 4c_1c_3}$, we obtain

$$V_1 = \frac{2c_3}{-c_2 + \sqrt{c_2^2 - 4c_1c_3}} < -\frac{2c_3}{c_2}.$$

Thus, $-c_2V_1 < 2c_3$. From Eq. (3.2), we get

$$c_1V_1^2 = -c_2V_1 - c_3 < c_3.$$

Therefore

$$\beta_1(1+\beta_2)V_1^2 + R_0 - 1 = c_1V_1^2 - c_3 < 0.$$

□

Theorem 3.4 *When the infected steady state E_1 of model (2.2) exists, E_1 is unstable for all $\tau \geq 0$.*

Proof (a) When $\tau = 0$, Eq. (3.6) becomes

$$\lambda^3 + (a_2 + b_2)\lambda^2 + (a_1 + b_1)\lambda + a_0 + b_0 = 0. \tag{3.11}$$

From the first equation of (3.1) and Lemma 3.3, we have

$$\begin{aligned} a_2 + b_2 &= \alpha_3 + \alpha_4 - \alpha_2 + R_0 > 0, \\ a_1 + b_1 &= (\alpha_3 + \alpha_4 - \alpha_2)R_0 + \alpha_3\beta_2V_1 > 0, \\ a_0 + b_0 &= \frac{\alpha_3\alpha_4}{1 + \beta_1V_1}\left[\beta_1(1+\beta_2)V_1^2 + R_0 - 1\right] < 0. \end{aligned}$$

From the existence of roots, we know that Eq. (3.11) has at least one positive root. Thus, E_1 is unstable when $\tau = 0$.

(b) When $\tau > 0$, the characteristic equation is

$$\lambda^3 + a_2\lambda^2 + a_1\lambda + a_0 + (b_2\lambda^2 + b_1\lambda + b_0)e^{-\lambda\tau} = 0, \tag{3.12}$$

where

$$\begin{aligned} a_2 &= \alpha_3 + \alpha_4 + R_0, \\ a_1 &= \alpha_3\alpha_4 + (\alpha_3 + \alpha_4)R_0, \\ a_0 &= \alpha_3\alpha_4R_0, \\ b_2 &= -\alpha_2, \\ b_1 &= \alpha_3(\beta_2V_1 - \alpha_4) - \alpha_2R_0, \\ b_0 &= \alpha_3\alpha_4V_1\left[\beta_2 + 1 - \frac{R_m}{(1+\beta_1V_1)^2}\right] - \alpha_3\alpha_4R_0. \end{aligned}$$

We have the following equation

$$h(z) = z^3 + mz^2 + lz + r = 0, \tag{3.13}$$

where

$$m = \alpha_3^2 + \alpha_4^2 + R_0^2 - \alpha_2^2 > 0,$$

$$
\begin{aligned}
l =& (\alpha_3^2 + \alpha_4^2 - \alpha_2^2)R_0^2 - 2\alpha_2\alpha_3\alpha_4 \frac{1}{1+\beta_1 V_1}[\beta_1(1+\beta_2)V_1^2 + R_0 - 1] \\
&+ 2\alpha_3\beta_2 V_1(\alpha_3\alpha_4 + \alpha_2 R_0) - \alpha_3^2\beta_2^2 V_1^2, \\
r =& (a_0 - b_0)(a_0 + b_0)
\end{aligned}
$$

and

$$
\begin{aligned}
a_0 + b_0 &= \frac{\alpha_3\alpha_4}{1+\beta_1 V_1}[\beta_1(1+\beta_2)V_1^2 + R_0 - 1], \\
a_0 - b_0 &= \frac{\alpha_3\alpha_4}{1+\beta_1 V_1}[R_0 + 1 + \beta_1 V_1(2R_0 - V_1(\beta_2 + 1))].
\end{aligned}
$$

From Lemma 3.3, we know that $\beta_1(1+\beta_2)V_1^2 + R_0 - 1 < 0$, which implies that $a_0 + b_0 < 0$. Additionally, we can derive that $\beta_1(1+\beta_2)V_1^2 < 1 - R_0 < 1 + R_0$, hence $a_0 - b_0 > 0$. Therefore, we obtain $r = (a_0 - b_0)(a_0 + b_0) < 0$. Consequently, Eq. (3.13) has one positive root z_0 for $m > 0$ and any l, leading to a positive root $\omega_0 = \sqrt{z_0}$.

In conclusion, the infected steady state E_1 is unstable for all $\tau \geq 0$. The proof is completed. □

At the infected steady state E_2, when $\tau = 0$, Eq. (3.6) becomes

$$
\lambda^3 + (a_2 + b_2)\lambda^2 + (a_1 + b_1)\lambda + a_0 + b_0 = 0, \tag{3.14}
$$

where

$$
\begin{aligned}
a_2 + b_2 &= \alpha_3 + \alpha_4 - \alpha_2 + R_0 > 0, \\
a_1 + b_1 &= (\alpha_3 + \alpha_4 - \alpha_2)R_0 + \alpha_3\beta_2 V_2 > 0, \\
a_0 + b_0 &= \frac{\alpha_3\alpha_4}{1+\beta_1 V_2}\left[\beta_1(1+\beta_2)V_2^2 + R_0 - 1\right].
\end{aligned}
$$

Lemma 3.5 *When E_2 exists, we have $\beta_1(1+\beta_2)V_2^2 + R_0 - 1 \geq 0$.*

Proof (a) When $R_0 \geq 1$, $\beta_1(1+\beta_2)V_2^2 + R_0 - 1 > 0$ always holds.

(b) When $R_0 < 1$, we know that $c_2 < 0$ and $\Delta = c_2^2 - 4c_1c_3 \geq 0$. Thus, $c_3 = 1 - R_0 > 0$. We have

$$
V_2 = \frac{-c_2 + \sqrt{c_2^2 - 4c_1c_3}}{2c_1}.
$$

Multiplying the numerator and denominator by $-c_2 - \sqrt{c_2^2 - 4c_1c_3}$, we obtain

$$
V_2 = \frac{2c_3}{-c_2 - \sqrt{c_2^2 - 4c_1c_3}} \geq -\frac{2c_3}{c_2}.
$$

Thus, $-c_2V_2 \geq 2c_3$. From Eq. (3.2) we get

$$
c_1V_2^2 = -c_2V_2 - c_3 \geq c_3.
$$

Therefore, we have

$$
\beta_1(1+\beta_2)V_2^2 + R_0 - 1 = c_1V_2^2 - c_3 \geq 0.
$$

The proof is completed. □

From Lemma 3.5, we obtain that $a_0 + b_0 \geq 0$. When $a_0 + b_0 = 0$, Eq. (3.14) has an eigenvalue of zero, indicating that a saddle-node bifurcation occurs at the infected steady state E_2. When $a_0 + b_0 > 0$, according to the Routh-Hurwitz criterion, the equation $\frac{\alpha_3\alpha_4}{1+\beta_1 V_2}\left[\beta_1(1+\beta_2)V_2^2 + R_0 - 1\right] < (\alpha_3 + \alpha_4 - \alpha_2 + R_0)[(\alpha_3 + \alpha_4 - \alpha_2)R_0 + \alpha_3\beta_2 V_2]$ holds when E_2 is stable.

When $\tau > 0$, let $i\omega$ ($\omega > 0$) be the root of the characteristic equation at E_2. We have

$$
h(z) = z^3 + mz^2 + lz + r = 0, \tag{3.15}
$$

where

$$
\begin{aligned}
m =& \alpha_3^2 + \alpha_4^2 + R_0^2 - \alpha_2^2 > 0, \\
l =& (\alpha_3^2 + \alpha_4^2 - \alpha_2^2)R_0^2 - 2\alpha_2\alpha_3\alpha_4 \frac{1}{1+\beta_1 V_2}[\beta_1(1+\beta_2)V_2^2 + R_0 - 1] \\
&+ 2\alpha_3\beta_2 V_2(\alpha_3\alpha_4 + \alpha_2 R_0) - \alpha_3^2\beta_2^2 V_2^2,
\end{aligned}
$$

$$r = (a_0 - b_0)(a_0 + b_0)$$

and

$$a_0 + b_0 = \frac{\alpha_3\alpha_4}{1+\beta_1 V_2}[\beta_1(1+\beta_2)V_2^2 + R_0 - 1],$$
$$a_0 - b_0 = \frac{\alpha_3\alpha_4}{1+\beta_1 V_2}[R_0 + 1 + \beta_1 V_2(2R_0 - V_2(\beta_2 + 1))].$$

From Lemma 3.5, we obtain that $a_0 + b_0 \geq 0$. When $a_0 + b_0 = 0$, Eq. (3.15) becomes $z(z^2 + mz + l) = 0$. In this case, Eq. (3.15) has a unique positive root $\omega_0 = \sqrt{z_0}$ if $l < 0$. When $a_0 + b_0 > 0$, we have $r = (a_0 - b_0)(a_0 + b_0) > 0$ if the equation has no positive roots. Thus, $a_0 - b_0 > 0$, which implies $R_0 + 1 + \beta_1 V_2(2R_0 - V_2(\beta_2 + 1)) > 0$. Therefore, the infected steady state E_2 is stable. Moreover, we have $R_0 + 1 + \beta_1 V_2(2R_0 - V_2(\beta_2 + 1)) < 0$ if $r < 0$. Then Eq. (3.15) has one positive root z_0 for $m > 0$ and any l, leading to a unique positive root $\omega_0 = \sqrt{z_0}$. Thus, we can conclude the following results.

Theorem 3.6 *(i) When $R_0 < 1$ and $\Delta = 0$, model (2.2) undergoes a saddle-node bifurcation at the infected steady state E_2.*
(ii) When $R_0 < 1$ and $\Delta > 0$, or $R_0 \geq 1$, if the following conditions hold:

(a) $\frac{\alpha_3\alpha_4}{1+\beta_1 V_2}\left[\beta_1(1+\beta_2)V_2^2 + R_0 - 1\right] < (\alpha_3 + \alpha_4 - \alpha_2 + R_0)[(\alpha_3 + \alpha_4 - \alpha_2)R_0 + \alpha_3\beta_2 V_2]$,
(b) $R_0 + 1 + \beta_1 V_2(2R_0 - V_2(\beta_2 + 1)) \geq 0$,

then the infected steady state E_2 of model (2.2) is locally asymptotically stable for all $\tau \geq 0$.

Theorem 3.7 *If the following conditions hold*

(i) $\frac{\alpha_3\alpha_4}{1+\beta_1 V_2}\left[\beta_1(1+\beta_2)V_2^2 + R_0 - 1\right] < (\alpha_3 + \alpha_4 - \alpha_2 + R_0)[(\alpha_3 + \alpha_4 - \alpha_2)R_0 + \alpha_3\beta_2 V_2]$,
(ii) $R_0 + 1 + \beta_1 V_2(2R_0 - V_2(\beta_2 + 1)) < 0$ *and* $l < 0$, *then E_2 is locally asymptotically stable when $\tau < \tau_0$ and unstable when $\tau > \tau_0$. Therefore, model (2.2) undergoes Hopf bifurcation when $\tau = \tau_0$,*

$$\tau_j = \frac{1}{\omega}\left(\arccos\left(\frac{(\omega^3 - a_1\omega)b_1\omega + (b_0 - b_2\omega^2)(a_2\omega^2 - a_0)}{(b_0 - b_2\omega^2)^2 + b_1^2\omega^2}\right) + 2j\pi\right), \quad j = 0, 1, 2, \ldots$$

Proof We need to verify the transversality condition for the Hopf bifurcation at $\tau = \tau_0$ [29], i.e., $\text{sign}\left(\text{Re}\left(\frac{d\lambda}{d\tau}\right)|_{\tau=\tau_0}\right) = \text{sign}\left(\frac{dh(z)}{dz}|_{z=\omega^2}\right)$. Taking the derivative of the Eq. (3.6) at τ, we obtain

$$\frac{dH(\lambda, \tau)}{d\tau} = \frac{\partial H(\lambda, \tau)}{\partial \tau} + \frac{\partial H(\lambda, \tau)}{\partial \lambda}\frac{d\lambda}{d\tau} = 0.$$

Then we have

$$\left(\frac{d\lambda}{d\tau}\right)^{-1} = -\frac{\frac{\partial H(\lambda,\tau)}{\partial \lambda}}{\frac{\partial H(\lambda,\tau)}{\partial \tau}} = \frac{(P_2'(\lambda) - \tau P_2(\lambda))e^{-\lambda\tau} + P_1'(\lambda)}{\lambda P_2(\lambda)e^{-\lambda\tau}}. \tag{3.16}$$

From $H(\lambda, \tau) = 0$ and $\lambda = i\omega$, we have

$$\left.\frac{d\lambda}{d\tau}\right|_{\tau=\tau_0}^{-1} = \frac{P_2'(i\omega)}{i\omega P_2(i\omega)} - \frac{\tau}{i\omega} - \frac{P_1'(i\omega)}{i\omega P_1(i\omega)}.$$

Next, from straightforward calculations, we can rewrite equation (3.15)

$$\begin{aligned} h(z) &= (a_0 - a_2 z)^2 + z(a_1 - z)^2 - (b_0 - b_2 z)^2 - z b_1^2 \\ &= A_1(z)^2 + zA_2(z)^2 - B_1(z)^2 - zB_2(z)^2 = 0. \end{aligned}$$

It follows that

$$\begin{aligned} \text{Re}\left(\left.\frac{d\lambda}{d\tau}\right|_{\tau=\tau_0}^{-1}\right) &= \text{Re}\left(\frac{P_2'(i\omega)}{i\omega P_2(i\omega)}\right) - \text{Re}\left(\frac{P_1'(i\omega)}{i\omega P_1(i\omega)}\right) \\ &= \frac{2A_1'A_1 + A_2^2 + 2zA_2'A_2}{A_1^2 + \omega^2 A_2^2} - \frac{2B_1'B_1 + B_2^2 + 2zB_2'B_2}{B_1^2 + \omega^2 B_2^2}. \end{aligned}$$

From $A_1(z)^2 + \omega^2 A_2(z)^2 = B_1(z)^2 + \omega^2 B_2(z)^2$, we obtain

$$\text{Re}\left(\left.\frac{d\lambda}{d\tau}\right|_{\tau=\tau_0}^{-1}\right) = \left.\frac{h'(z)}{B_1^2 + \omega^2 B_2^2}\right|_{z=\omega^2}. \tag{3.17}$$

Table 1 Parameter values of model (2.1)

Parameters	Values	Description	References
Λ	10 $mm^{-3}day^{-1}$	Generation rate of uninfected cells	[26]
ε	0.01 day^{-1}	Maximum homeostatic growth rate	[25]
M	300 copies mm^{-3}	Homeostatic half-velocity	[25]
k	4.57×10^{-5} mm^3 day^{-1}	Rate of cell-free virus infection	[21]
β	1.5×10^{-4} $mm^3 day^{-1}$	Rate of cell-to-cell transmission	[12]
p	40 virions per cell day^{-1}	Rate of viral production	[21]
δ	0.01 day^{-1}	Death rate of infected cells that Have not started to produce virus	[3]
d_1	0.02 day^{-1}	Death rate of uninfected cells	[26]
d_2	0.4 day^{-1}	Death rate of infected cells	[26]
d_3	2.4 day^{-1}	Clearance rate of free virus	[21]

We know that $B_1(z)^2 + \omega^2 B_2(z)^2 > 0$, which leads to

$$\operatorname{sign}\left(\operatorname{Re}\left(\frac{\mathrm{d}\lambda}{\mathrm{d}\tau}\right)\Big|_{\tau=\tau_0}\right) = \operatorname{sign}\left(\frac{dh(z)}{\mathrm{d}z}\Big|_{z=\omega^2}\right).$$

This completes the proof. □

4 Direction and stability of the Hopf bifurcation

To better understand the Hopf bifurcation, we investigate the direction and stability of the bifurcating periodic solutions using the normal form method and center manifold theories, as described by Hassard [30]. We obtain the following results (see Appendix for proof).

Theorem 4.1 *Under the condition of Theorem* 3.7,

(i) if $\mu_2 > 0$ (or $\mu_2 < 0$), the Hopf bifurcation is supercritical (or subcritical) and the bifurcated periodic solutions exist for $\tau > \tau_0$ (or $\tau < \tau_0$),
(ii) if $\gamma > 0$ (or $\gamma < 0$), then the bifurcated periodic solutions are unstable (or stable),
(iii) if $T_2 > 0$ (or $T_2 < 0$), then the period of the bifurcated periodic solutions increases (or decreases).

5 Numerical results

In this section, we illustrate the analytical results through numerical simulations, focusing particularly on the effects of cell homeostatic proliferation and cell-to-cell transmission on HIV infection. We have fixed the values of $\alpha_1 = 16.71$, $\alpha_2 = 3.29$, $\alpha_3 = 20$, $\alpha_4 = 120$, $\beta_1 = 1.46$, and $\beta_2 = 0.19$, as calculated from Table 1.

For our simulations, we set $R_0 = 0.5$ and varied the values of τ and R_m. Figure 1 demonstrates that the infection-free steady state $E_0 = (0.5, 0, 0)$ is locally asymptotically stable with the initial conditions $(T(0), I(0), V(0)) = (2, 1, 1)$, in accordance with Theorem 3.2. As shown in Fig. 1a, variations in τ can reduce the peak of infection but prolong the time taken for the infection to dissipate. Altering the value of R_m does not affect the time until the infection disappears but does increase the peak of infection, as illustrated in Fig. 1b.

We incorporated cell-to-cell transmission into the model to study its impact on HIV infection. To examine the effects of varying the cell-to-cell transmission rate (β), we adjusted the parameters related to β in model (2.2), specifically R_0, α_1, α_2, and β_2. Which requires assurance $R_0 < 1$. As shown in Fig. 2, we observe that the peak of infection increases with the cell-to-cell transmission rate at the infection-free steady state. This suggests that the number of infected cells escalates rapidly within a short period, resulting in a significant increase in infection levels.

Model (2.2) undergoes both a backward bifurcation and a saddle-node bifurcation at the infected steady state E_2. In Fig. 3, a backward bifurcation (BP) occurs when $R_0 \leq 1$, indicating the presence of two infected steady states. This suggests that even if R_0 is less than 1, sustained infection transmission may still occur, which has significant implications for public health policy. At $R_0 = 0.979$, model (2.2) undergoes a saddle-node bifurcation (LP(SN)) with multiplicity 2. When the backward bifurcation occurs, the curve below the saddle-node represents an unstable equilibrium, while the curve above indicates a stable equilibrium.

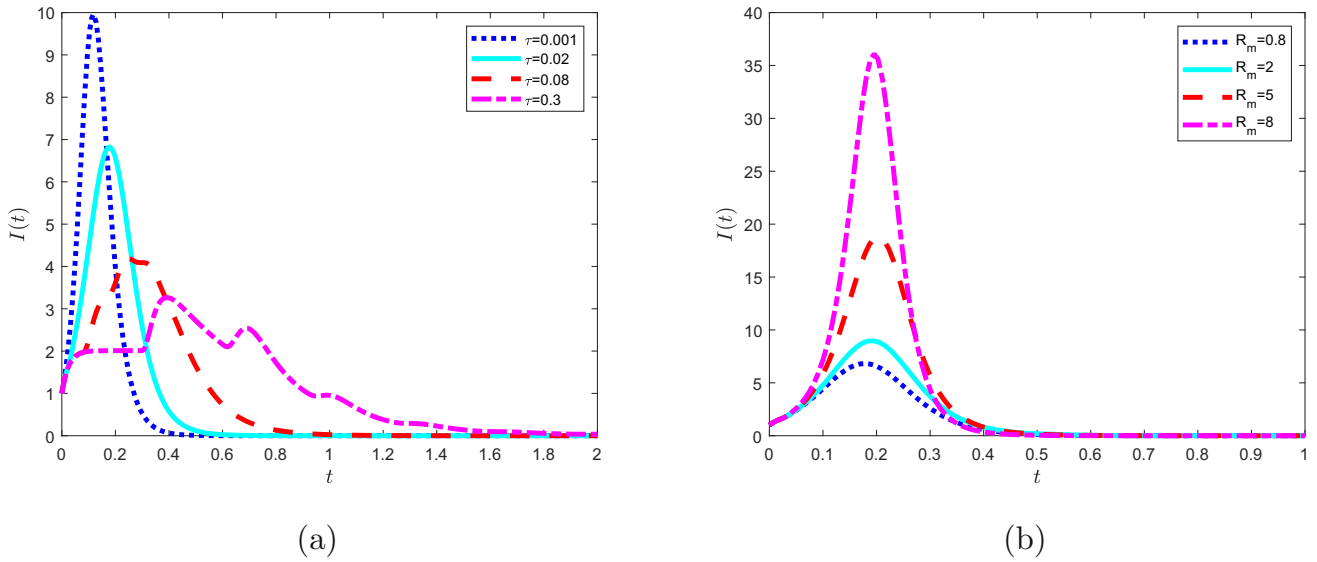

Fig. 1 The infection-free steady state E_0 is locally asymptotically stable when $R_0 = 0.5$. **a** The evolution of $I(t)$ for E_0 is shown with different values of τ: the short blue dotted line, light blue solid line, long red dotted line, and magenta dotted line represent the dynamics of $I(t)$ under $\tau = 0.001$, $\tau = 0.02$, $\tau = 0.08$, and $\tau = 0.3$, respectively. **b** The evolution of $I(t)$ for E_0 is shown with different values of R_m: the short blue dotted line, light blue solid line, long red dotted line, and magenta dotted line represent the dynamics of $I(t)$ under $R_m = 0.8$, $R_m = 2$, $R_m = 5$, and $R_m = 8$, respectively

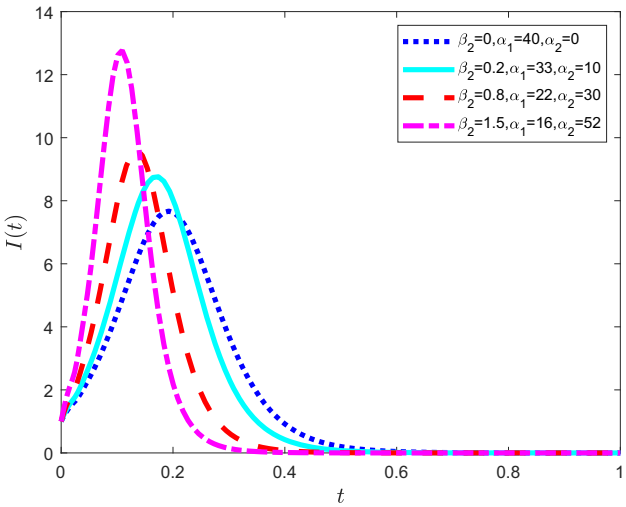

Fig. 2 The infection-free steady state E_0 is locally asymptotically stable at different values of the cell-to-cell transmission rate when $R_m = 0.8$. The short blue dotted line represents $\beta_2 = 0$, $\alpha_1 = 40$, and $\alpha_2 = 0$; the light blue solid line represents $\beta_2 = 0.2$, $\alpha_1 = 33$, and $\alpha_2 = 10$; the long red dotted line represents $\beta_2 = 0.8$, $\alpha_1 = 22$, and $\alpha_2 = 30$; and the magenta dotted line represents $\beta_2 = 1.5$, $\alpha_1 = 16$, and $\alpha_2 = 52$

Figure 4 illustrates the Hopf bifurcation curve and changes in stability under different parameters for $\tau = 0$. Figure 4a depicts the Hopf bifurcation curve on the $R_m - R_0$ parameter plane. Above this curve, the steady state E_2 is stable, while below it, E_2 is unstable. Figure 4b–d show the relationships between R_m and T, I, and V when $R_m = 16$ and $R_0 = 2$, respectively. The results indicate that a Hopf bifurcation occurs at $R_m = 16.027$, changing the stability of the infected steady state $E_2 = (1, 17.665, 17.665)$. As R_m increases, model (2.2) transitions from stable (blue curve) to unstable (red curve).

The infected steady state $E_2 = (1, 1.857, 1.857)$ is locally asymptotically stable for various values of τ, given the initial conditions $(T(0), I(0), V(0)) = (2, 1, 1)$, in accordance with Theorem 3.6. In Fig. 5a, when $R_0 = 2$ and $R_m = 1.5$, the peak value of infection decreases as τ increases, whereas the time to reach the steady state lengthens with an increase in τ. Figure 5b illustrates that at $\tau = 0.03$, as homeostatic proliferation (R_m) increases, not only does the magnitude of the infected steady state E_2 increase, but the time to reach this steady state also extends. This demonstrates that homeostatic proliferation (R_m) has a more significant impact on HIV infection dynamics than the delay (τ).

Similarly, to assess the impact of cell-to-cell transmission on the infected steady state, it is necessary to vary the cell-to-cell transmission rate. With fixed values of $R_m = 1.5$, $\beta_1 = 0.73$, and $\tau = 0.02$, we modified the values of α_1, α_2, and β_2. Of note, setting α_2 and β_2 to zero eliminates cell-to-cell transmission. Our observations indicate that as the cell-to-cell transmission rate increases, the peak of the infected steady state also rises, while the time required to reach the steady state decreases, as shown in Fig. 6.

Fig. 3 The backward bifurcation and saddle-node bifurcation occur at the infected steady state E_2

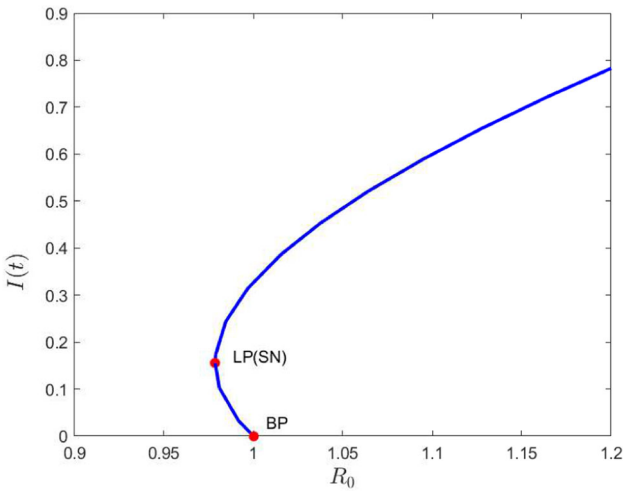

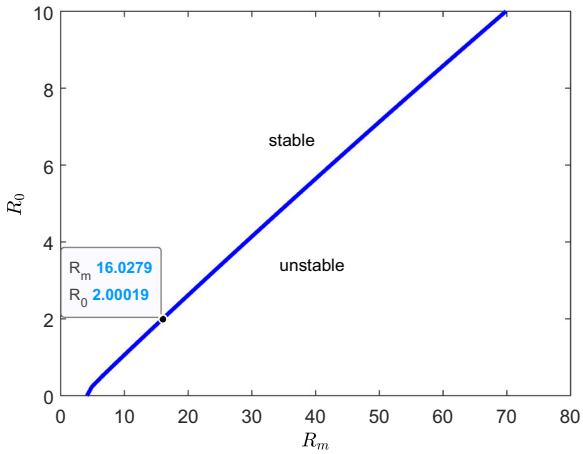

(a) $\tau = 0$

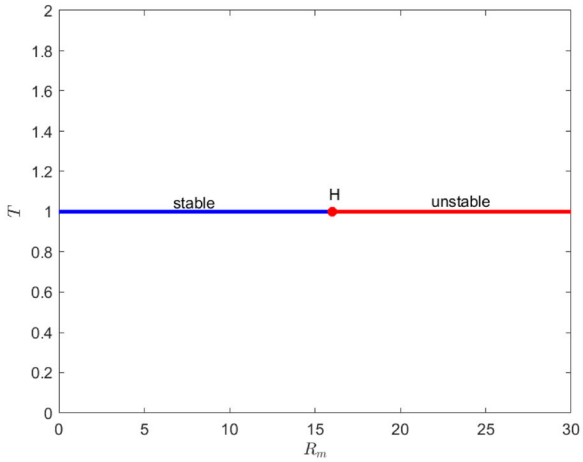

(b) $R_0 = 2$

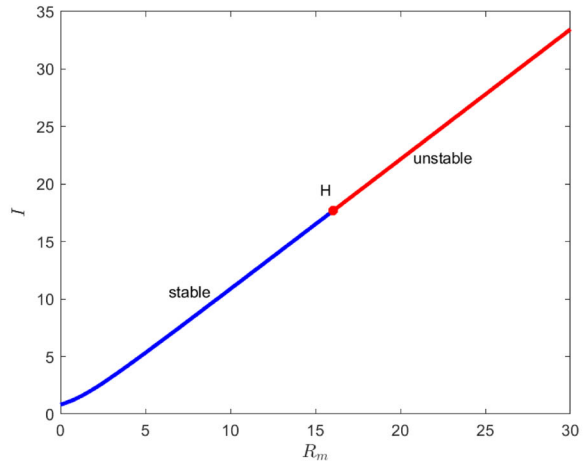

(c) $R_0 = 2$

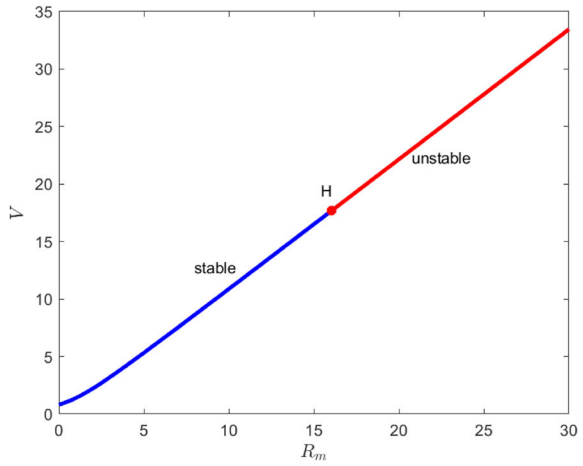

(d) $R_0 = 2$

Fig. 4 **a** The Hopf bifurcation curve in $(R_m,\ R_0)$ parameter plane. The components T, I and V of infected steady state E_2 with respect to the parameter R_m when $R_0 = 2$ in **b**, **c** and **d**, respectively

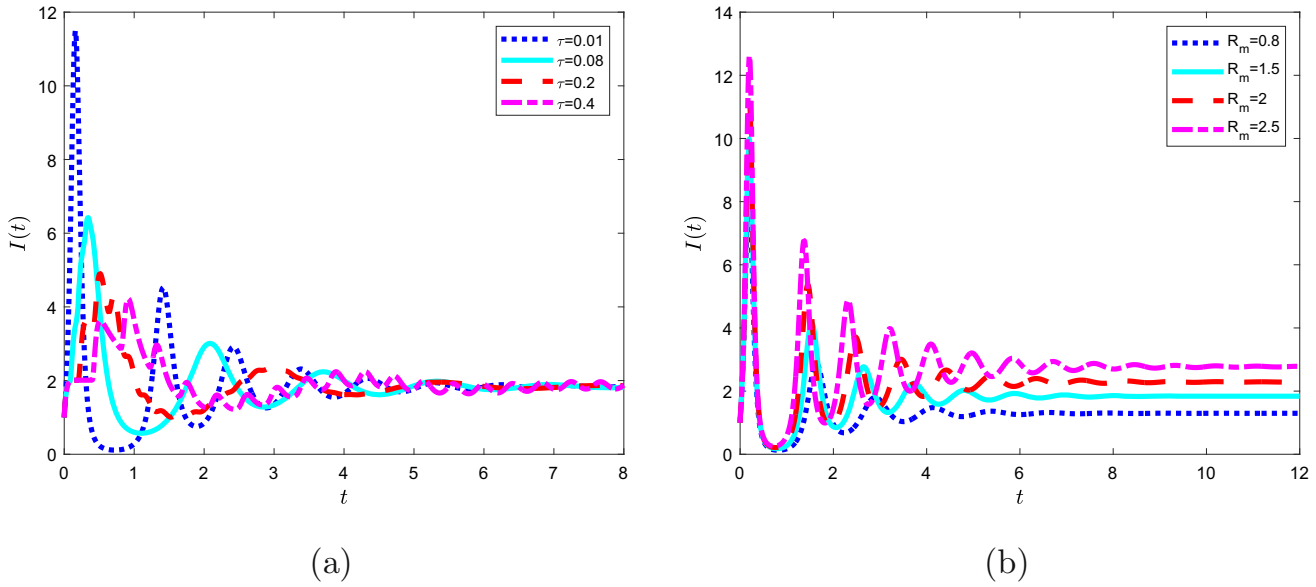

Fig. 5 The infected steady state E_2 is locally asymptotically stable when $R_0 = 2$. **a** The evolution of $I(t)$ for E_2 is shown with different values of τ when $R_m = 1.5$: the short blue dotted line, light blue solid line, long red dotted line, and magenta dotted line represent the dynamics of $I(t)$ under $\tau = 0.01$, $\tau = 0.08$, $\tau = 0.2$, and $\tau = 0.4$, respectively. **b** The evolution of $I(t)$ for E_2 is shown with different values of R_m when $\tau = 0.03$: the short blue dotted line, light blue solid line, long red dotted line, and magenta dotted line represent the dynamics of $I(t)$ under $R_m = 0.8$, $R_m = 1.5$, $R_m = 2$, and $R_m = 2.5$, respectively

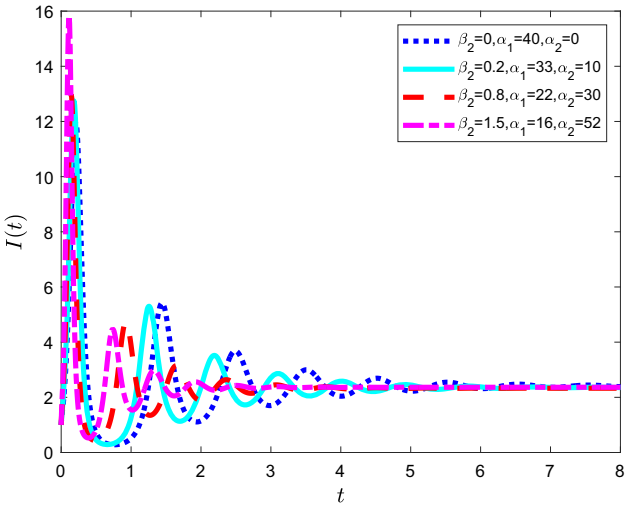

Fig. 6 The infected steady state E_2 is locally asymptotically stable at different values of the cell-to-cell transmission rate when $R_m = 1.5$. The short blue dotted line represents $\beta_2 = 0$, $\alpha_1 = 40$, and $\alpha_2 = 0$; the light blue solid line represents $\beta_2 = 0.2$, $\alpha_1 = 33$, and $\alpha_2 = 10$; the long red dotted line represents $\beta_2 = 0.8$, $\alpha_1 = 22$, and $\alpha_2 = 30$; and the magenta dotted line represents $\beta_2 = 1.5$, $\alpha_1 = 16$, and $\alpha_2 = 52$

When $R_0 = 3$ and $R_m = 5$, the infected steady state E_2 exists. As shown in Fig. 7, this steady state is stable at $\tau = 0.03$ and becomes unstable at $\tau = 0.06$. Thus, the stability of model (2.2) changes from stable to unstable as τ increases. To identify the critical value for Hopf bifurcation, Fig. 8 shows how the difference between the maximum and minimum values of uninfected cells $T(t)$ varies with τ. When this difference is zero, it indicates that the steady state has reached a stable condition; if the difference is nonzero, it signifies that the steady state is experiencing oscillations. Model (2.2) begins to exhibit bifurcation at $\tau_0 = 0.055$. In accordance with Theorem 3.7, this transition from stability to instability through a Hopf bifurcation indicates that E_2 undergoes a supercritical Hopf bifurcation at $\tau = \tau_0$.

Next, we investigate how the Hopf bifurcation behavior of model (2.2) changes with variations in parameters τ, R_m and R_0. We show the Hopf bifurcation curves for different values of $\tau = 0.001, 0.005, 0.01, 0.05, 0.1$ in Fig. 9a. The infected steady state E_2 is stable above these curves and unstable below them. It is also observed that the Hopf bifurcation curves tend to approximate a straight line as τ increases. In Fig. 9b, we illustrate the effect of homeostatic proliferation on model (2.2) and plot the Hopf bifurcation curves for various values of $R_m = 5, 5.5, 6, 6.5, 7$. Similarly, the infected steady state E_2 is stable above the Hopf bifurcation curves and becomes unstable below them. The results indicate that the stable region for E_2 decreases while the unstable region expands as τ and R_m increase. These Hopf bifurcation curves allow us to understand the dynamic characteristics of the model under different parameter combinations, providing valuable insights for understanding and predicting virus transmission.

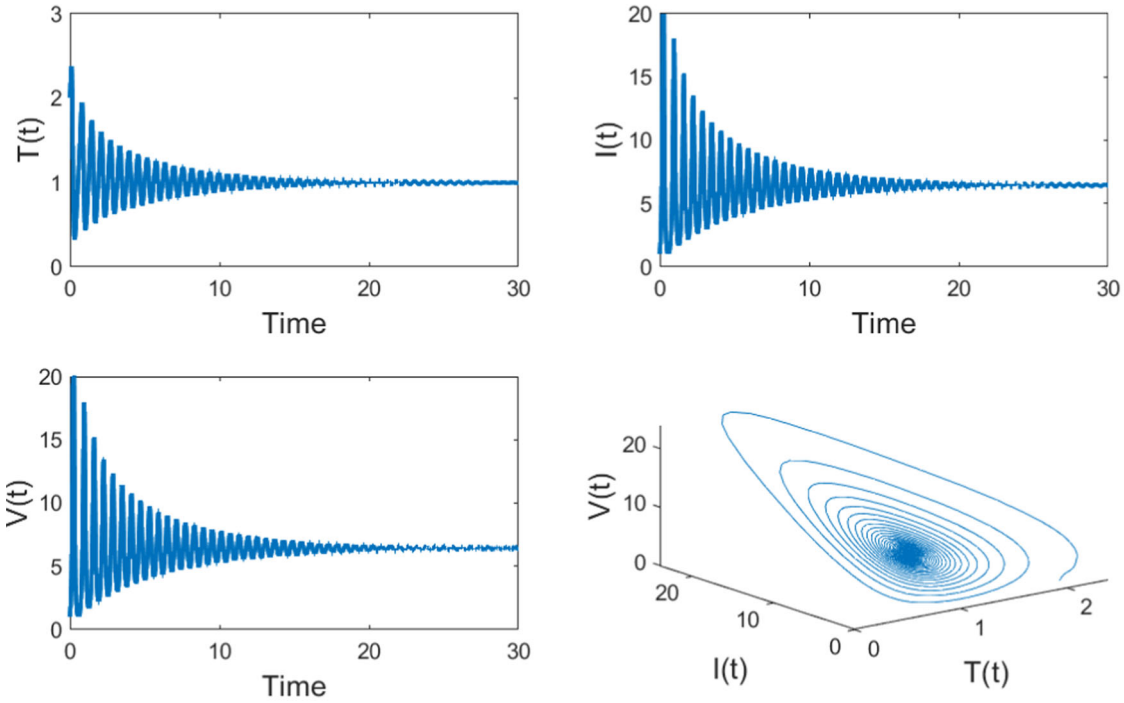

(a) E_2 is locally asymptotically stable at $\tau = 0.03$.

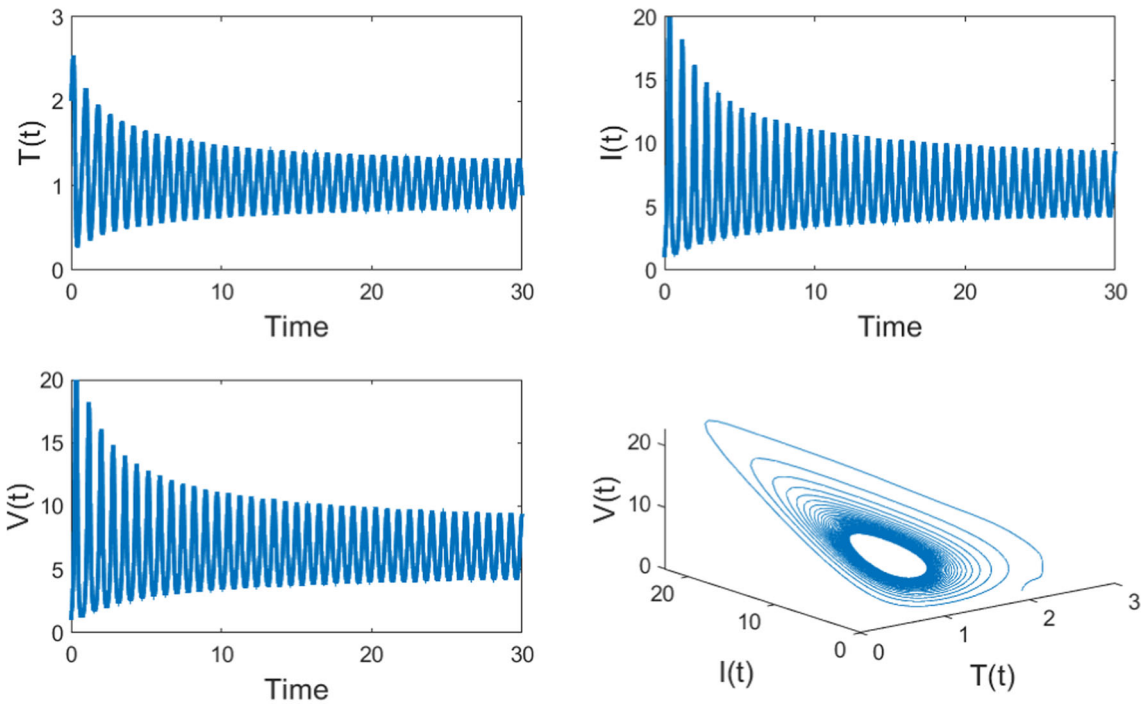

(b) E_2 is unstable at $\tau = 0.06$.

Fig. 7 The evolution of solution curves and phase portraits associated with the infected steady state E_2 are shown with initial conditions $(T(0), I(0), V(0)) = (2, 1, 1)$ when $R_0 = 3$ and $R_m = 5$

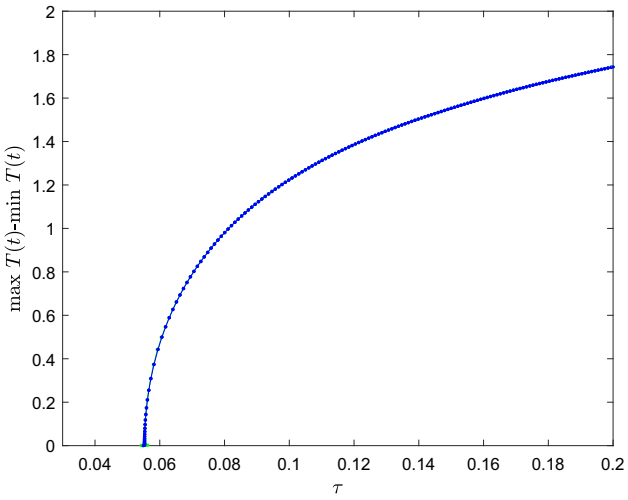

Fig. 8 A Hopf bifurcation occurs at $\tau = 0.0552895$ when $R_0 = 3$ and $R_m = 5$. Vertical axis: if the difference between the maximum and minimum values of uninfected cells $T(t)$ is nonzero, it indicates that model (2.2) is experiencing oscillations

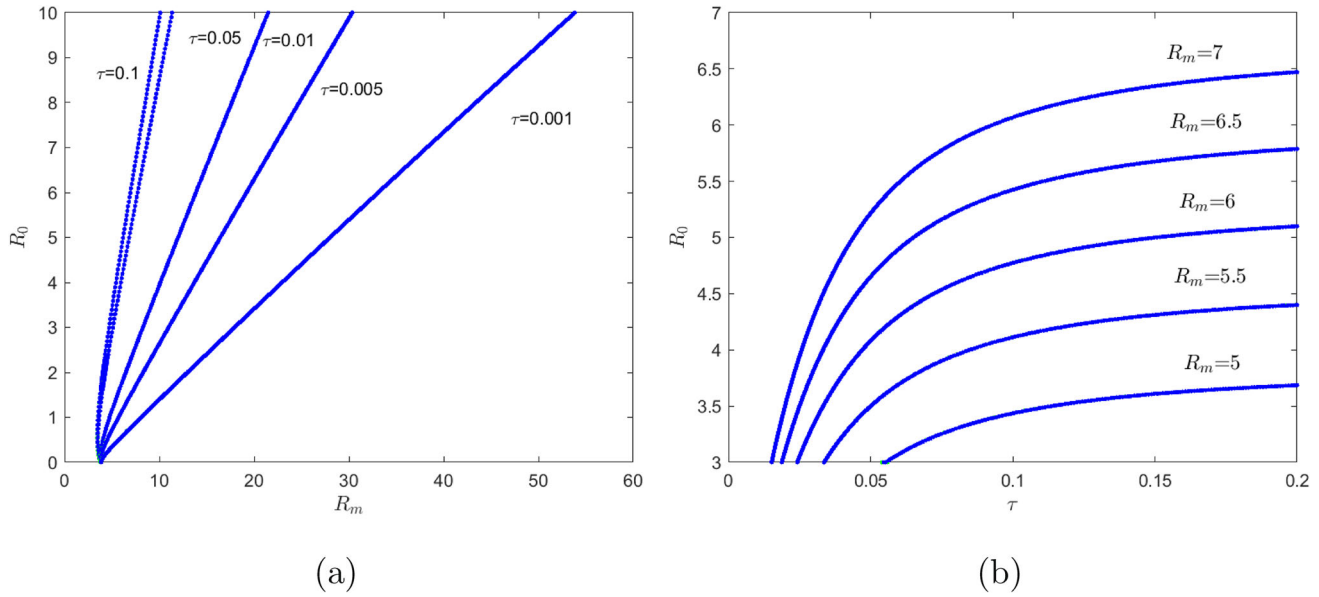

Fig. 9 The Hopf bifurcation curves of model (2.2). **a** The Hopf bifurcation curves in (R_m, R_0) parameter plane with different values of τ. **b** The Hopf bifurcation curves in (τ, R_0) parameter plane with different values of R_m

Cell-to-cell transmission is a critical factor in this study, essential for understanding its impact on the model dynamics. Figure 10 displays the Hopf bifurcation curves for cell-to-cell transmission when $R_m = 5$ and $\tau = 0.1$. The red curve represents the Hopf bifurcation without cell-to-cell transmission, while the blue curve represents the Hopf bifurcation with cell-to-cell transmission. The infected steady state E_2 is unstable above the Hopf bifurcation curve and stable below it. This indicates that the stable region for E_2 expands and the unstable region contracts as the cell-to-cell transmission rate increases. This is consistent with Figs. 2 and 6, which show a decrease in the time required for the infected steady state E_2 to reach stability.

6 Conclusion and discussion

Since the discovery of the first HIV/AIDS case in the 1980s, we have been engaged in a battle against HIV for about 40 years [31]. Due to the complexity of disease transmission, it is necessary to continually refine models to better reflect reality. The homeostatic proliferation of cells is a significant factor influencing disease spread, resulting in complex dynamical behaviors in the model. This paper primarily focuses on the proliferative effect induced by free virus on uninfected cells, which can help maintain the stability of uninfected cell numbers in the circulatory system [21, 32].

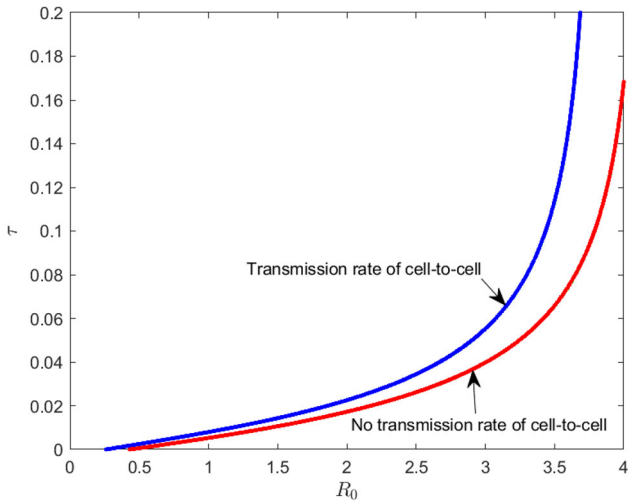

Fig. 10 The Hopf bifurcation curves in the $(R_0,\ \tau)$ parameter plane of model (2.2) are shown with and without cell-to-cell transmission. The blue line represents the case with cell-to-cell transmission, and the red line represents the case without it

This paper establishes a delayed model with homeostatic proliferation and cell-to-cell transmission. We transform the model and prove its positivity, and we discuss the existence of its steady states. When $R_0 < 1$ and $\Delta = 0$, model (2.2) undergoes a saddle-node bifurcation, resulting in two infected steady states (E_1 and E_2) in addition to the infection-free steady state (E_0). The infection-free steady state is stable when $R_0 < 1$; otherwise, it is unstable. The infected steady state E_1 is always unstable. We analyze the local stability conditions of E_2, the conditions for Hopf bifurcation, and the direction and stability of these bifurcations. Numerical results show that when $R_0 < 1$, E_0 is stable for any τ and R_m, leading to eventual disease extinction. However, backward bifurcation and saddle-node bifurcation can occur in model (2.2). It is observed that the time delay τ, homeostatic proliferation R_m, and cell-to-cell transmission β all influence HIV infection. In Figs. 9 and 10, the infected steady state E_2 transitions from a stable to an unstable state, indicating that the disease exhibits periodic recurrence, complicating eradication efforts. Some previous models did not consider homeostatic proliferation, while others assumed logistic growth. Logistic growth affects the rate of disease spread without altering its dynamic behavior [33, 34].

Homeostatic proliferation alters the model's dynamic behavior, making it essential to inhibit free virus during preventive treatment. Current treatments typically include protease inhibitors and reverse transcriptase inhibitors, as studied in modeling studies [35, 36]. However, to mitigate the effects of cellular homeostatic proliferation, it may also be necessary to develop drugs that can block the proliferation of uninfected cells stimulated by free virus. Such targeted interventions could help reduce the activation of uninfected cells and improve the effectiveness of treatment strategies [37].

In summary, this paper investigates how homeostatic proliferation and cell-to-cell transmission can cause the model to transition from stable to unstable, complicating the prevention and treatment of the virus. Since this study only analyzes the effects of homeostatic proliferation under a time-delay model, it is important to recognize that viral infection is influenced by multiple factors. For example, the age of cell infection, immune response, and preventive treatment measures all impact viral infection [5, 38, 39]. In addition to the effects of drugs on the virus, the role of the innate immune system should be taken into account, highlighting an area that requires further research.

Acknowledgements X. Wang was supported by the National Natural Science Foundation of China (No. 12171413), the Natural Science Foundation of Henan Province (222300420016). Y. Wang was supported by the Scientific Research Foundation of Graduate School of Xinyang Normal University (No. 2024KYJJ059). L. Rong was supported by the NSF Grant DMS-2324692.

Data Availibility Statement The data that support the findings of this study are available from the corresponding author upon reasonable request. The manuscript has associated data in a data repository.

Appendix

At $E_2 = (1,\ I_2,\ V_2)$, we have $I_2 = V_2$. Let $X(t) = T(\tau t) - 1,\ \ Y(t) = I(\tau t) - I_2,\ \ Z(t) = V(\tau t) - V_2$ and $\tau = \tau_0 + \mu,\ \ \mu \in R$. Model (2.2) can be written as a functional differential equation system in $C = C([-1,\ 0],\ R^3)$ as

$$\dot{x}(t) = L_\mu(x_t) + f(\mu, x_t), \tag{6.1}$$

where $x(t) = (X(t),\ Y(t),\ Z(t))^T \in R^3$, $L_\mu : C \to R^3$, $f : R \times C \to R^3$. We can define an operator as $\phi(\theta) = (\phi_1(\theta),\ \phi_2(\theta),\ \phi_3(\theta))^T \in C$. We get the linear part

$$\begin{aligned} L_\mu(\phi) =& (\tau_0+\mu)\begin{pmatrix} \frac{R_m}{1+\beta_1 V_2}V_2 - \beta_2 V_2 - V_2 - 1 & -\beta_2 & \frac{R_m}{(1+\beta_1 V_2)^2} - 1 \\ 0 & -\alpha_3 & 0 \\ 0 & \alpha_4 & -\alpha_4 \end{pmatrix}\begin{pmatrix}\phi_1(0)\\ \phi_2(0)\\ \phi_3(0)\end{pmatrix} \\ &+ (\tau_0+\mu)\begin{pmatrix} 0 & 0 & 0 \\ \alpha_3 V_2 & \alpha_2 & \alpha_1 \\ 0 & 0 & 0 \end{pmatrix}\begin{pmatrix}\phi_1(-1)\\ \phi_2(-1)\\ \phi_3(-1)\end{pmatrix}. \end{aligned} \tag{6.2}$$

The nonlinear part is

$$f(\mu,\phi) = (\tau_0+\mu)\begin{pmatrix} \left(\frac{R_m}{(1+\beta_1 V_2)^2} - 1\right)\phi_1(0)\phi_3(0) - \beta_2\phi_1(0)\phi_2(0) - \frac{\beta_1 R_m}{(1+\beta_1 V_2)^3}\phi_3^2(0) \\ \alpha_1\phi_1(-1)\phi_3(-1) + \alpha_2\phi_1(-1)\phi_2(-1) \\ 0 \end{pmatrix}. \tag{6.3}$$

By the Riesz representation theorem, there exists a matrix $\eta(\theta,\ \mu) \in [-1,\ 0] \to R^3$ of bounded variation, such that

$$L_\mu(\phi) = \int_{-1}^{0} \mathrm{d}\eta(\theta,\mu)\phi(\theta) \quad \text{for } \phi \in C. \tag{6.4}$$

We can choose

$$\begin{aligned} \eta(\theta,\mu) =& (\tau_0+\mu)\begin{pmatrix} \frac{R_m}{1+\beta_1 V_2}V_2 - \beta_2 V_2 - V_2 - 1 & -\beta_2 & \frac{R_m}{(1+\beta_1 V_2)^2} - 1 \\ 0 & -\alpha_3 & 0 \\ 0 & \alpha_4 & -\alpha_4 \end{pmatrix}\delta(\theta) \\ &- (\tau_0+\mu)\begin{pmatrix} 0 & 0 & 0 \\ \alpha_3 V_2 & \alpha_2 & \alpha_1 \\ 0 & 0 & 0 \end{pmatrix}\delta(\theta+1), \end{aligned} \tag{6.5}$$

where $\delta(\theta)$ is Dirac delta function.

Define

$$A(\mu)\phi(\theta) = \begin{cases} \frac{\mathrm{d}\phi(\theta)}{\mathrm{d}\theta}, & \theta \in [-1,\ 0), \\ \int_{-1}^{0} \mathrm{d}\eta(\mu,\ s)\phi(s), & \theta = 0 \end{cases}$$

and

$$R(\mu)\phi(\theta) = \begin{cases} 0, & \theta \in [-1,\ 0), \\ f(\mu,\ \phi), & \theta = 0. \end{cases}$$

To conveniently study the Hopf bifurcation, we rewrite the system (6.1) as

$$\dot{x}_t = A(\mu)x_t + R(\mu)x_t, \tag{6.6}$$

where $x_t = x(t+\theta),\ \theta \in [-1,\ 0]$. The adjoint operator A^* of A is defined by

$$A^*\varphi(s) = \begin{cases} -\frac{\mathrm{d}\varphi}{ds}, & s \in (0,\ 1], \\ \int_{-1}^{0} \mathrm{d}\eta^T(t,\ 0)\varphi(-t), & s = 0, \end{cases}$$

where η^T is the transpose of the matrix η and $\varphi \in C^1([0,\ 1],\ R^{3*})$, R^{3*} is complex vector space of dimension 3. Then for $\phi \in C([-1,\ 0],\ R^3)$, we can define a bilinear form

$$\langle\varphi(s),\phi(\theta)\rangle = \bar{\varphi}(0)\phi(0) - \int_{\theta=-1}^{0}\int_{\xi=0}^{\theta} \bar{\varphi}^T(\xi-\theta)\mathrm{d}\eta(\theta)\phi(\xi), \tag{6.7}$$

where $\eta(\theta) = \eta(\theta, 0)$ and $\bar{\varphi}(0)\phi(0)$ means $\sum_{i=1}^{3} \bar{\varphi}_i(0)\phi_i(0)$. From the discussion in the previous section, we know that $\pm i\omega_0\tau_0$ are eigenvalues of $A(0)$ and other eigenvalues are all negative real parts. Moreover, $\pm i\omega_0\tau_0$ are also eigenvalues of A^*.

Next, we calculate the eigenvector of $A(0)$ and A^* corresponding to $i\omega_0\tau_0$ and $-i\omega_0\tau_0$, respectively. Let $q(\theta) = (1, u, v)^T e^{i\omega_0\tau_0\theta}$, $\theta \in (-1, 0]$. Form the above discussion, we have $A(0)q(\theta) = i\omega_0\tau_0 q(\theta)$. Thus, we get

$$\tau_0 \begin{pmatrix} i\omega_0 - \frac{R_m}{1+\beta_1 V_2} V_2 + \beta_2 V_2 + V_2 + 1 & \beta_2 & 1 - \frac{R_m}{(1+\beta_1 V_2)^2} \\ -\alpha_3 V_2 e^{-i\omega_0\tau_0} & i\omega_0 + \alpha_3 - \alpha_2 e^{-i\omega_0\tau_0} & -\alpha_1 e^{-i\omega_0\tau_0} \\ 0 & -\alpha_4 & i\omega_0 + \alpha_4 \end{pmatrix} \begin{pmatrix} 1 \\ u \\ v \end{pmatrix} = \begin{pmatrix} 0 \\ 0 \\ 0 \end{pmatrix}.$$

By straightforward calculations, we obtain

$$u = \frac{(i\omega_0 + \alpha_4)v}{\alpha_4},$$
$$v = \frac{\alpha_3\alpha_4 V_2 e^{-i\omega_0\tau_0}}{-\omega_0^2 + \alpha_3\alpha_4 + (\alpha_3\omega_0 + \alpha_4\omega_0 - \alpha_2 e^{-i\omega_0\tau_0}\omega_0)i - \alpha_3\alpha_4 e^{-i\omega_0\tau_0}}.$$

Similarly, we let $q^*(s) = D(1, u^*, v^*)^T e^{i\omega_0\tau_0 s}$, $s \in [0, 1)$ and $A^* q^*(s) = -i\omega_0\tau_0 q^*(s)$. We obtain

$$\tau_0 \begin{pmatrix} -i\omega_0 - \frac{R_m}{1+\beta_1 V_2} V_2 + \beta_2 V_2 + V_2 + 1 & -\alpha_3 V_2 e^{i\omega_0\tau_0} & 0 \\ \beta_2 & -i\omega_0 + \alpha_3 - \alpha_2 e^{i\omega_0\tau_0} & -\alpha_4 \\ 1 - \frac{R_m}{(1+\beta_1 V_2)^2} & -\alpha_1 e^{i\omega_0\tau_0} & -i\omega_0 + \alpha_4 \end{pmatrix} \begin{pmatrix} 1 \\ u^* \\ v^* \end{pmatrix} = \begin{pmatrix} 0 \\ 0 \\ 0 \end{pmatrix},$$

which leads to

$$u^* = \frac{-R_m V_2 + (\beta_2 V_2 + V_2 + 1 - i\omega_0)(1 + \beta_1 V_2)}{\alpha_3 V_2 (1 + \beta_1 V_2) e^{i\omega_0\tau_0}},$$
$$v^* = \frac{\beta_2 + (\alpha_3 - \alpha_2 e^{i\omega_0\tau_0} - i\omega_0)u^*}{\alpha_4}.$$

The condition $\langle q^*, q\rangle = 1$ needs to be satisfied, which can obtain the value of D. From (6.7), we have

$$\begin{aligned} \langle q^*(s), q(\theta)\rangle &= \bar{D}(1 + u\bar{u^*} + v\bar{v^*}) - \int_{\theta=-1}^{0} \int_{\xi=0}^{\theta} \bar{D}(1, \bar{u^*}, \bar{v^*}) e^{-i\omega_0\tau_0(\xi-\theta)} \mathrm{d}\eta(\theta)(1, u, v)^T e^{i\omega_0\tau_0\xi} \mathrm{d}\xi \\ &= \bar{D}(1 + u\bar{u^*} + v\bar{v^*}) - \int_{\theta=-1}^{0} \bar{D}(1, \bar{u^*}, \bar{v^*}) \theta e^{i\omega_0\tau_0\theta} \mathrm{d}\eta(\theta)(1, u, v)^T \\ &= \bar{D}(1 + u\bar{u^*} + v\bar{v^*}) + \bar{D}\tau_0(1, \bar{u^*}, \bar{v^*}) \begin{pmatrix} 0 & 0 & 0 \\ \alpha_3 V_2 & \alpha_2 & \alpha_1 \\ 0 & 0 & 0 \end{pmatrix} \begin{pmatrix} 1 \\ u \\ v \end{pmatrix} e^{-i\omega_0\tau_0} \\ &= \bar{D}[1 + u\bar{u^*} + v\bar{v^*} + \tau_0(\alpha_3 V_2 \bar{u^*} + \alpha_2 u\bar{u^*} + \alpha_1 \bar{u^*} v) e^{-i\omega_0\tau_0}] = 1. \end{aligned}$$

Thus, we get

$$\bar{D} = [1 + u\bar{u^*} + v\bar{v^*} + \tau_0(\alpha_3 V_2 \bar{u^*} + \alpha_2 u\bar{u^*} + \alpha_1 \bar{u^*} v) e^{-i\omega_0\tau_0}]^{-1}.$$

Therefore,

$$D = [1 + \bar{u}u^* + \bar{v}v^* + \tau_0(\alpha_3 V_2 u^* + \alpha_2 \bar{u}u^* + \alpha_1 u^* \bar{v}) e^{i\omega_0\tau_0}]^{-1}.$$

We first construct the coordinates describing the center manifold M_μ at $\mu = 0$. Let x_t be the solution of system (6.6) when $\mu = 0$.

Define

$$z(t) = \langle q^*, x_t\rangle, \quad W(t, \theta) = x_t(\theta) - z(t)q(\theta) - \bar{z}(t)\bar{q}(\theta). \tag{6.8}$$

On the center manifold M_0, we have

$$W(t, \theta) = W(z, \bar{z}, \theta),$$

where

$$W(z, \bar{z}, \theta) = W_{20}(\theta)\frac{z^2}{2} + W_{11}(\theta)z\bar{z} + W_{02}(\theta)\frac{\bar{z}^2}{2} + W_{30}(\theta)\frac{z^3}{6} + \cdots, \tag{6.9}$$

and z and $\bar{z}$ are local coordinates for center manifold M_0 in the direction of q and q^*, respectively. We need to consider real solutions. For solution $x_t \in M_0$ of (6.6), we have

$$\dot{z}(t) = \langle q^*, \dot{x}_t \rangle = i\omega_0\tau_0 z + \bar{q}^*(0) f_0(z, \bar{z}), \tag{6.10}$$

where $f_0(z, \bar{z}) = f(0, W(z, \bar{z}, \theta) + z(t)q(\theta) + \bar{z}(t)\bar{q}(\theta))$. Then we have

$$f_0 = f_{20}\frac{z^2}{2} + f_{11}z\bar{z} + f_{02}\frac{\bar{z}^2}{2} + f_{21}\frac{z^2\bar{z}}{2} + \cdots.$$

Rewrite equation (6.10) as

$$\dot{z}(t) = i\omega_0\tau_0 z + g(z, \bar{z}),$$

where

$$g(z, \bar{z}) = \bar{q}^*(0) f_0(z, \bar{z}) = g_{20}\frac{z^2}{2} + g_{11}z\bar{z} + g_{02}\frac{\bar{z}^2}{2} + g_{21}\frac{z^2\bar{z}}{2} + \cdots.$$

From (6.8) and (6.9), we have

$$\begin{aligned} x_t(\theta) &= W(t, \theta) + z(t)q(\theta) + \bar{z}(t)\bar{q}(\theta) \\ &= W_{20}(\theta)\frac{z^2}{2} + W_{11}(\theta)z\bar{z} + W_{02}(\theta)\frac{\bar{z}^2}{2} + (1, u, v)^T e^{i\omega_0\tau_0\theta} z + (1, \bar{u}, \bar{v})^T e^{-i\omega_0\tau_0\theta}\bar{z} + \cdots. \end{aligned} \tag{6.11}$$

Thus, we obtain

$$\begin{aligned} g(z, \bar{z}) &= \bar{q}^*(0) f_0(z, \bar{z}) \\ &= \tau_0\bar{D}(1, \bar{u^*}, \bar{v^*}) \begin{pmatrix} \left(\frac{R_m}{(1+\beta_1 V_2)^2} - 1\right) x_{1t}(0)x_{3t}(0) - \beta_2 x_{1t}(0)x_{2t}(0) - \frac{\beta_1 R_m}{(1+\beta_1 V_2)^3} x_{3t}^2(0) \\ \alpha_1 x_{1t}(-1)x_{3t}(-1) + \alpha_2 x_{1t}(-1)x_{2t}(-1) \\ 0 \end{pmatrix} \\ &= \tau_0\bar{D}\left\{\left(\frac{R_m}{(1+\beta_1 V_2)^2} - 1\right) x_{1t}(0)x_{3t}(0) - \beta_2 x_{1t}(0)x_{2t}(0) - \frac{\beta_1 R_m}{(1+\beta_1 V_2)^3} x_{3t}^2(0) \right. \\ &\quad \left. + \bar{u^*}\alpha_1 x_{1t}(-1)x_{3t}(-1) + \bar{u^*}\alpha_2 x_{1t}(-1)x_{2t}(-1)\right\}, \end{aligned}$$

where $x_t(\theta) = (x_{1t}(\theta), x_{2t}(\theta), x_{3t}(\theta))^T = W(t, \theta) + z(t)q(\theta) + \bar{z}(t)\bar{q}(\theta)$. We have

$$\begin{aligned} x_{1t}(0) &= z + \bar{z} + W_{20}^{(1)}(0)\frac{z^2}{2} + W_{11}^{(1)}(0)z\bar{z} + W_{02}^{(1)}(0)\frac{\bar{z}^2}{2} + o(|(z, \bar{z})|^3), \\ x_{2t}(0) &= uz + \bar{u}\bar{z} + W_{20}^{(2)}(0)\frac{z^2}{2} + W_{11}^{(2)}(0)z\bar{z} + W_{02}^{(2)}(0)\frac{\bar{z}^2}{2} + o(|(z, \bar{z})|^3), \\ x_{3t}(0) &= vz + \bar{v}\bar{z} + W_{20}^{(3)}(0)\frac{z^2}{2} + W_{11}^{(3)}(0)z\bar{z} + W_{02}^{(3)}(0)\frac{\bar{z}^2}{2} + o(|(z, \bar{z})|^3), \\ x_{1t}(-1) &= ze^{-i\omega_0\tau_0} + \bar{z}e^{i\omega_0\tau_0} + W_{20}^{(1)}(-1)\frac{z^2}{2} + W_{11}^{(1)}(-1)z\bar{z} + W_{02}^{(1)}(-1)\frac{\bar{z}^2}{2} + o(|(z, \bar{z})|^3), \\ x_{2t}(-1) &= uze^{-i\omega_0\tau_0} + \bar{u}\bar{z}e^{i\omega_0\tau_0} + W_{20}^{(2)}(-1)\frac{z^2}{2} + W_{11}^{(2)}(-1)z\bar{z} + W_{02}^{(2)}(-1)\frac{\bar{z}^2}{2} + o(|(z, \bar{z})|^3), \\ x_{3t}(-1) &= vze^{-i\omega_0\tau_0} + \bar{v}\bar{z}e^{i\omega_0\tau_0} + W_{20}^{(3)}(-1)\frac{z^2}{2} + W_{11}^{(3)}(-1)z\bar{z} + W_{02}^{(3)}(-1)\frac{\bar{z}^2}{2} + o(|(z, \bar{z})|^3). \end{aligned}$$

Comparing the coefficients, we get

$$
\begin{aligned}
g_{20} =& 2\tau_0\bar{D}\left[\left(\frac{R_m}{(1+\beta_1V_2)^2}-1\right)v-\beta_2u-\frac{\beta_1R_m}{(1+\beta_1V_2)^3}v^2+\alpha_1\bar{u^*}ve^{-2i\omega_0\tau_0}+\alpha_2\bar{u^*}ue^{-2i\omega_0\tau_0}\right],\\
g_{11} =& \tau_0\bar{D}\left[\left(\frac{R_m}{(1+\beta_1V_2)^2}-1\right)(v+\bar{v})-\beta_2(u+\bar{u})-2\frac{\beta_1R_m}{(1+\beta_1V_2)^3}v\bar{v}\right.\\
&\left.+\alpha_1\bar{u^*}(v+\bar{v})+\alpha_2\bar{u^*}(u+\bar{u})\right],\\
g_{02} =& 2\tau_0\bar{D}\left[\left(\frac{R_m}{(1+\beta_1V_2)^2}-1\right)\bar{v}-\beta_2\bar{u}-\frac{\beta_1R_m}{(1+\beta_1V_2)^3}\bar{v}^2+\alpha_1\bar{u^*}\bar{v}e^{2i\omega_0\tau_0}+\alpha_2\bar{u^*}\bar{u}e^{2i\omega_0\tau_0}\right],\\
g_{21} =& \tau_0\bar{D}\left(\frac{R_m}{(1+\beta_1V_2)^2}-1\right)\left(2vW_{11}^{(1)}(0)+\bar{v}W_{20}^{(1)}(0)+W_{20}^{(3)}(0)+2W_{11}^{(3)}(0)\right)\\
&-\tau_0\bar{D}\beta_2\left(2uW_{11}^{(1)}(0)+\bar{u}W_{20}^{(1)}(0)+W_{20}^{(2)}(0)+2W_{11}^{(2)}(0)\right)\\
&-\tau_0\bar{D}\frac{\beta_1R_m}{(1+\beta_1V_2)^3}\left(2\bar{v}W_{20}^{(3)}(0)+4vW_{11}^{(3)}(0)\right)\\
&+\tau_0\bar{D}\alpha_1\bar{u^*}\left(2ve^{-i\omega_0\tau_0}W_{11}^{(1)}(-1)+\bar{v}e^{i\omega_0\tau_0}W_{20}^{(1)}(-1)+e^{i\omega_0\tau_0}W_{20}^{(3)}(-1)+2e^{-i\omega_0\tau_0}W_{11}^{(3)}(-1)\right)\\
&+\tau_0\bar{D}\alpha_2\bar{u^*}\left(2ue^{-i\omega_0\tau_0}W_{11}^{(1)}(-1)+\bar{u}e^{i\omega_0\tau_0}W_{20}^{(1)}(-1)+e^{i\omega_0\tau_0}W_{20}^{(2)}(-1)+2e^{-i\omega_0\tau_0}W_{11}^{(2)}(-1)\right).
\end{aligned}
$$

Next, we need to get the values of $W_{20}(\theta)$ and $W_{11}(\theta)$ to calculate g_{21}. From (6.6) and (6.8), we obtain

$$
\dot{W}=\dot{x}_t-\dot{z}q-\dot{\bar{z}}\bar{q}=\begin{cases}A(0)W-gq(\theta)-\bar{g}\bar{q}(\theta), & \theta\in[-1,0),\\ A(0)W-gq(0)-\bar{g}\bar{q}(0)+f_0, & \theta=0.\end{cases}\tag{6.12}
$$

By Eq. (6.9), we obtain

$$
\begin{aligned}
\dot{W} =& \dot{W}_z\dot{z}+\dot{W}_{\bar{z}}\dot{\bar{z}}\\
=& (W_{20}(\theta)z+W_{11}(\theta)\bar{z}+\cdots)(i\omega_0\tau_0z(t)+g(z,\bar{z}))\\
&+(W_{11}(\theta)z+W_{02}(\theta)\bar{z}+\cdots)(-i\omega_0\tau_0\bar{z}(t)+\bar{g}(z,\bar{z})).
\end{aligned}\tag{6.13}
$$

Substituting (6.9) and (6.13) in (6.12), and comparing coefficients of $\frac{z^2}{2}$ and $z\bar{z}$, we get

$$
(2i\omega_0\tau_0I-A(0))W_{20}(\theta)=\begin{cases}-g_{20}q(\theta)-\bar{g}_{02}\bar{q}(\theta), & \theta\in[-1,0),\\ -g_{20}q(0)-\bar{g}_{02}\bar{q}(0)+f_{20}, & \theta=0\end{cases}\tag{6.14}
$$

and

$$
-A(0)W_{11}(\theta)=\begin{cases}-g_{11}q(\theta)-\bar{g}_{11}\bar{q}(\theta), & \theta\in[-1,0),\\ -g_{11}q(0)-\bar{g}_{11}\bar{q}(0)+f_{11}, & \theta=0.\end{cases}\tag{6.15}
$$

From the definition of $A(0)$ when $\theta\in[-1,0)$, (6.14) and (6.15), we get

$$
\dot{W}_{20}=2i\omega_0\tau_0W_{20}(\theta)+g_{20}q(\theta)+\bar{g}_{02}\bar{q}(\theta)
$$

and

$$
\dot{W}_{11}=g_{11}q(\theta)+\bar{g}_{11}\bar{q}(\theta).
$$

Therefore, we have

$$
W_{20}(\theta)=\frac{ig_{20}}{\omega_0\tau_0}q(0)e^{i\omega_0\tau_0\theta}+\frac{i\bar{g}_{02}}{3\omega_0\tau_0}\bar{q}(0)e^{-i\omega_0\tau_0\theta}+G_1e^{2i\omega_0\tau_0\theta},\tag{6.16}
$$

$$
W_{11}(\theta)=-\frac{ig_{11}}{\omega_0\tau_0}q(0)e^{i\omega_0\tau_0\theta}+\frac{i\bar{g}_{11}}{\omega_0\tau_0}\bar{q}(0)e^{-i\omega_0\tau_0\theta}+G_2,\tag{6.17}
$$

where $G_i=(G_i^{(1)},G_i^{(2)},G_i^{(3)})^T\in R^3$, $i=1,2$.

Next, we calculate the values of G_1 and G_2. From the definition of $A(0)$ and (6.14), we have

$$
\int_{-1}^{0}\mathrm{d}\eta(\theta)W_{20}(\theta)=2i\omega_0\tau_0W_{20}(\theta)+g_{20}q(0)+\bar{g}_{02}\bar{q}(0)-f_{20}.\tag{6.18}
$$

Substituting (6.16) in (6.18) and noticing that

$$\left(i\omega_0\tau_0 I - \int_{-1}^{0} e^{i\omega_0\tau_0\theta}\mathrm{d}\eta(\theta)\right)q(0) = 0$$

and

$$\left(-i\omega_0\tau_0 I - \int_{-1}^{0} e^{-i\omega_0\tau_0\theta}\mathrm{d}\eta(\theta)\right)\bar{q}(0) = 0,$$

we have

$$\left(2i\omega_0\tau_0 I - \int_{-1}^{0} e^{2i\omega_0\tau_0\theta}\mathrm{d}\eta(\theta)\right)G_1 = 2\tau_0\begin{pmatrix}\left(\frac{R_m}{(1+\beta_1V_2)^2}-1\right)v - \beta_2 u - \frac{\beta_1 R_m}{(1+\beta_1V_2)^3}v^2\\ \alpha_1 v e^{-2i\omega_0\tau_0} + \alpha_2 u e^{-2i\omega_0\tau_0}\\ 0\end{pmatrix}.$$

It follows that

$$\begin{pmatrix}2i\omega_0 - \frac{R_m}{1+\beta_1V_2}V_2 + \beta_2V_2 + V_2 + 1 & \beta_2 & 1 - \frac{R_m}{(1+\beta_1V_2)^2}\\ -\alpha_3V_2e^{-2i\omega_0\tau_0} & 2i\omega_0 + \alpha_3 - \alpha_2e^{-2i\omega_0\tau_0} & -\alpha_1e^{-2i\omega_0\tau_0}\\ 0 & -\alpha_4 & 2i\omega_0 + \alpha_4\end{pmatrix}G_1$$
$$= 2\begin{pmatrix}\left(\frac{R_m}{(1+\beta_1V_2)^2}-1\right)v - \beta_2 u - \frac{\beta_1 R_m}{(1+\beta_1V_2)^3}v^2\\ \alpha_1 v e^{-2i\omega_0\tau_0} + \alpha_2 u e^{-2i\omega_0\tau_0}\\ 0\end{pmatrix}.$$

Therefore, the following value of G_1 is given

$$G_1 = 2\begin{pmatrix}2i\omega_0 - \frac{R_m}{1+\beta_1V_2}V_2 + \beta_2V_2 + V_2 + 1 & \beta_2 & 1 - \frac{R_m}{(1+\beta_1V_2)^2}\\ -\alpha_3V_2e^{-2i\omega_0\tau_0} & 2i\omega_0 + \alpha_3 - \alpha_2e^{-2i\omega_0\tau_0} & -\alpha_1e^{-2i\omega_0\tau_0}\\ 0 & -\alpha_4 & 2i\omega_0 + \alpha_4\end{pmatrix}^{-1}$$
$$\begin{pmatrix}\left(\frac{R_m}{(1+\beta_1V_2)^2}-1\right)v - \beta_2 u - \frac{\beta_1 R_m}{(1+\beta_1V_2)^3}v^2\\ \alpha_1 v e^{-2i\omega_0\tau_0} + \alpha_2 u e^{-2i\omega_0\tau_0}\\ 0\end{pmatrix}.$$

Similarly, from (6.17), we obtain

$$\int_{-1}^{0}\mathrm{d}\eta(\theta)G_2 = -2\tau_0\begin{pmatrix}\left(\frac{R_m}{(1+\beta_1V_2)^2}-1\right)(v+\bar{v}) - \beta_2(u+\bar{u}) - 2\frac{\beta_1 R_m}{(1+\beta_1V_2)^3}v\bar{v}\\ \alpha_1(v+\bar{v}) + \alpha_2(u+\bar{u})\\ 0\end{pmatrix}.$$

We have

$$\begin{pmatrix}\frac{R_m}{1+\beta_1V_2}V_2 - \beta_2V_2 - V_2 - 1 & -\beta_2 & \frac{R_m}{(1+\beta_1V_2)^2} - 1\\ \alpha_3V_2 & \alpha_2 - \alpha_3 & \alpha_1\\ 0 & \alpha_4 & -\alpha_4\end{pmatrix}G_2$$
$$= 2\begin{pmatrix}\left(1 - \frac{R_m}{(1+\beta_1V_2)^2}\right)(v+\bar{v}) + \beta_2(u+\bar{u}) + 2\frac{\beta_1 R_m}{(1+\beta_1V_2)^3}v\bar{v}\\ -\alpha_1(v+\bar{v}) - \alpha_2(u+\bar{u})\\ 0\end{pmatrix}.$$

Therefore, the following value of G_2 is given

$$G_2 = 2\begin{pmatrix}\frac{R_m}{1+\beta_1V_2}V_2 - \beta_2V_2 - V_2 - 1 & -\beta_2 & \frac{R_m}{(1+\beta_1V_2)^2} - 1\\ \alpha_3V_2 & \alpha_2 - \alpha_3 & \alpha_1\\ 0 & \alpha_4 & -\alpha_4\end{pmatrix}^{-1}$$
$$\begin{pmatrix}\left(1 - \frac{R_m}{(1+\beta_1V_2)^2}\right)(v+\bar{v}) + \beta_2(u+\bar{u}) + 2\frac{\beta_1 R_m}{(1+\beta_1V_2)^3}v\bar{v}\\ -\alpha_1(v+\bar{v}) - \alpha_2(u+\bar{u})\\ 0\end{pmatrix}.$$

Thus, we can obtain $W_{20}(\theta)$ and $W_{11}(\theta)$.

From the values of g_{20}, g_{11}, g_{02} and g_{21}, the following parameters can be calculated:

$$
\begin{aligned}
c_1(0) &= \frac{i}{2\omega_0\tau_0}\left(g_{11}g_{20} - 2|g_{11}|^2 - \frac{|g_{02}|^2}{3}\right) + \frac{g_{21}}{2},\\
\mu_2 &= -\frac{\mathrm{Re}\{c_1(0)\}}{\mathrm{Re}\{\lambda'(\tau_0)\}},\\
\gamma &= 2\mathrm{Re}\{c_1(0)\},\\
T_2 &= -\frac{\mathrm{Im}\{c_1(0)\} + \mu_2\mathrm{Im}\{\lambda'(\tau_0)\}}{\omega_0\tau_0}.
\end{aligned}
$$

References

1. World Health Organization: HIV. Revised June 2023. Available from https://www.who.int/zh/news-room/fact-sheets/detail/hiv-aids
2. A. Raza, A. Ahmadian, M. Rafiq et al., Modeling the effect of delay strategy on transmission dynamics of HIV/AIDS disease. Adv. Differ. Equ. **2020**(1), 1–13 (2020)
3. A. Alshorman, X. Wang, M. Joseph Meyer et al., Analysis of HIV models with two time delays. J. Biol. Dyn. **11**(sup1), 40–64 (2017)
4. P. Jia, J. Yang, X. Li, Optimal control and cost-effective analysis of an age-structured emerging infectious disease model. Infect. Dis. Model. **7**(1), 149–169 (2022)
5. X. Wang, Y. Lou, X. Song, Age-structured within-host HIV dynamics with multiple target cells. Stud. Appl. Math. **138**(1), 43–76 (2017)
6. I. Sadowski, F.B. Hashemi, Strategies to eradicate HIV from infected patients: elimination of latent provirus reservoirs. Cell. Mol. Life Sci. **76**, 3583–3600 (2019)
7. B. Monel, E. Beaumont, D. Vendrame et al., HIV cell-to-cell transmission requires the pro-duction of infectious virus particles and does not proceed through env-mediated fusion pores. J. Virol. **86**(7), 3924–3933 (2012)
8. J.M. Timpe, Z. Stamataki, A. Jennings et al., Hepatitis C virus cell-cell transmission in hepatoma cells in the presence of neutralizing antibodies. Hepatology **47**(1), 17–24 (2008)
9. C. Qin, X. Wang, L. Rong, An age-structured model of HIV latent infection with two transmission routes: analysis and optimal control. Complexity **2020**, 1–22 (2020)
10. X. Wang, S. Tang, X. Song et al., Mathematical analysis of an HIV latent infection model including both virus-to-cell infection and cell-to-cell transmission. J. Biol. Dyn. **11**(sup2), 455–483 (2017)
11. A. Alshorman, N. Al-Hosainat, T. Jackson, Analysis of HIV latent infection model with multiple infection stages and different drug classes. J. Biol. Dyn. **16**(1), 713–732 (2022)
12. K. Hattaf, N. Yousfi, Modeling the adaptive immunity and both modes of transmission in HIV infection. Computation **6**(2), 37 (2018)
13. P.K. Roy, A.N. Chatterjee, D. Greenhalgh, Q.J.A. Khan, Long term dynamics in a mathematical model of HIV-1 infection with delay in different variants of the basic drug therapy model. Nonlinear Anal. Real World Appl. **14**(3), 1621–1633 (2013)
14. S. Ghosh, A.K. Roy, P.K. Roy, Implementation of suitable optimal control strategy through introspection of different delay induced mathematical models for leprosy: a comparative study. Opt. Control Appl. Methods **45**, 336–361 (2024)
15. T. Igarashi, Y. Endo, G. Englund et al., Emergence of a highly pathogenic simian/human immunodeficiency virus in a rhesus macaque treated with anti-CD8 mAb during a primary infection with a nonpathogenic virus. Proc. Natl. Acad. Sci. **96**(24), 14049–14054 (1999)
16. S. Pankavich, N. Neri, D. Shutt, Bistable dynamics and Hopf bifurcation in a refined model of early stage HIV infection. Discrete Contin. Dyn. Syst. B **25**(8), 2867–2893 (2020)
17. C.L. Mackall, F.T. Hakim, R.E. Gress, Restoration of T-cell homeostasis after T-cell depletion. Semin. Immunol. **9**(6), 339–346 (1997)
18. C. Tanchot, M.M. Rosado, F. Agenes et al., Lymphocyte homeostasis. Semin. Immunol. **9**(6), 331–337 (1997)
19. X. Fan, C.M. Brauner, L. Wittkop, Mathematical analysis of a HIV model with quadratic logistic growth term. Discrete Contin. Dyn. Syst. B **17**(7), 2359–2385 (2012)
20. M. Catalfamo, C. Wilhelm, L. Tcheung et al., CD4 and CD8 T cell immune activation during chronic HIV infection: roles of homeostasis, HIV, type I IFN, and IL-7. J. Immunol. **186**(4), 2106–2116 (2011)
21. M.M. Hadjiandreou, R. Conejeros, V.S. Vassiliadis, Towards a long-term model construction for the dynamic simulation of HIV infection. Math. Biosci. Eng. **4**(3), 489–504 (2007)
22. Q. Xu, J. Huang, Y. Dong et al., A delayed HIV infection model with the homeostatic proliferation of CD4+ T cells. Acta Math. Appl. Sin. Engl. Ser. **38**(2), 441–462 (2022)
23. T. Loudon, S. Pankavich, Mathematical analysis and dynamic active subspaces for a long term model of HIV. Math. Biosci. Eng. **14**(3), 709–733 (2017)
24. B. Levy, H.E. Correia, F. Chirove et al., Modeling the effect of HIV/AIDS stigma on HIV infection dynamics in Kenya. Bull. Math. Biol. **83**, 1–25 (2021)
25. E.A. Hernandez-Vargas, R.H. Middleton, Modeling the three stages in HIV infection. J. Theor. Biol. **320**, 33–40 (2013)
26. A.S. Perelson, D.E. Kirschner, R. De Boer, Dynamics of HIV infection of CD4+ T cells. Math. Biosci. **114**(1), 81–125 (1993)
27. K. Guo, W. Ma, R. Qiang, Global dynamics analysis of a time-delayed dynamic model of Kawasaki disease pathogenesis. Discrete Contin. Dyn. Syst. Ser. B **27**(4), 2367–2400 (2022)
28. P. Van den Driessche, J. Watmough, Reproduction numbers and sub-threshold endemic equilibria for compartmental models of disease transmission. Math. Biosci. **180**(1–2), 29–48 (2002)
29. Y. Kuang, *Delay Differential Equations: With Applications in Population Dynamics* (Academic Press, London, 1993)
30. B.D. Hassard, N.D. Kazarinoff, Y.H. Wan, *Theory and Applications of Hopf Bifurcation* (Cambridge University Press, Cambridge, 1981)
31. C. Beyrer, A pandemic anniversary: 40 years of HIV/AIDS. The Lancet **397**(10290), 2142–2143 (2021)
32. S. Prakash, A.K. Umrao, P.K. Srivastava, Dynamical model of HIV infection with homeostatic growth of CD4+ T cells and immune response. Int. J. Biomath. **66**, 2450026 (2024)
33. N. Akbari, R. Asheghi, Optimal control of an HIV infection model with logistic growth, celluar and homural immune response, cure rate and cell-to-cell spread. Bound. Value Probl. **2022**(1), 5 (2022)

34. N. Akbari, R. Asheghi, M. Nasirian, Stability and dynamic of HIV-1 mathematical model with logistic target cell growth, treatment rate, cure rate and cell-to-cell spread. Taiwan. J. Math. **26**(2), 411–441 (2022)
35. L. Xue, K. Zhang, H. Wang, Long-term forecast of HIV/AIDS epidemic in China with fear effect and 90–90–90 strategies. Bull. Math. Biol. **84**(11), 132 (2022)
36. T. Guo, Z. Qiu, L. Rong, A within-host drug resistance model with continuous state-dependent viral strains. Appl. Math. Lett. **104**, 106223 (2020)
37. L. Beilina, M. Eriksson, I. Gainova, Time-adaptive determination of drug efficacy in mathematical model of HIV infection. Differ. Equ. Dyn. Syst. **32**(1), 313–347 (2024)
38. T. Guo, Z. Qiu, K. Kitagawa et al., Modeling HIV multiple infection. J. Theor. Biol. **509**, 110502 (2021)
39. R.J. De Boer, A.S. Perelson, Target cell limited and immune control models of HIV infection: a comparison. J. Theor. Biol. **190**(3), 201–214 (1998)